AMP Deaminase 3 overexpression regulates cellular energetics and signaling for PGC-1α activation.

by

Spencer Miller

May, 2017

Director of Thesis: Jeffrey J. Brault

Major Department: Kinesiology

Skeletal muscles undergoing atrophy have decreased [ATP], PGC-1α expression, and mitochondrial content. This combination of findings is unexpected because decreased [ATP] is often associated with greater [AMP] and subsequent activation of AMPK, a known inducer of PGC-1α activity and mitochondrial biogenesis. A possible explanation is increased enzyme activity of AMP Deaminase 3 ($AMP \rightarrow IMP + NH_3$), which is highly overexpressed in atrophic muscles and functions to prevent increases in [AMP]. We tested the hypothesis that AMPD3 overexpression would significantly attenuate DNP (mitochondria uncoupler) induced phosphorylation of AMPK(Thr172) and PGC-1α promotor activity through regulation of intracellular energetics (ATP, ADP, AMP). **Methods:** Myotubes were transduced with adenoviruses encoding AMPD3 or GFP (control) and then treated for 1 h with 0.6mM 2,4 dinitrophenol (DNP). Nucleotides, amino acids, and proteins were extracted immediately after DNP treatment and measured by UPLC and Western Blot. To confirm DNP was not toxic, myotubes were washed, and samples were collected 1 h later for nucleotides and amino acids. To determine the effect of AMPD3 overexpression on PGC-1α promotor activity we transfected myoblasts with a 2kb PGC-1α promotor-luciferase reporter plasmid. After 5 days of AMPD3 or

GFP overexpression and a 4-day 100μM DNP treatment, we measured luciferase activity. We also stained myotubes for mitochondria using a green fluorescent dye (MitoTracker green FM) and quantified the percentage of pixels positive for florescence. **Results:** DNP treatment resulted in a 40% decline in [ATP], and increased [ADP] (1.4-fold), [AMP] (13.8-fold), AMP:ATP ratio (24-fold), and [IMP] (from undetectable) ($p<0.001$). DNP treatment also significantly increased phosphorylated AMPK(Thr172) (6.1-fold), and phosphorylation of downstream AMPK targets, ACC (Ser79, 4.8-fold) and ULK1 (Ser555, 2-fold) ($p<0.001$). Aspartic acid levels increased 7.1-fold ($p<0.001$), suggesting decreased activity of the purine nucleotide cycle (IMP + aspartic acid →→ AMP). As expected, myotubes that were overexpressing AMPD3 had significantly attenuated increases in [ADP] (1.1-fold), [AMP] (5.3-fold), and the AMP:ATP ratio (9.6-fold) ($p<0.001$), and this was reflected by significantly less phosphorylated AMPK(Thr172) ($p<0.05$). No changes were measured in aspartic acid or phosphorylation of ACC(Ser79) and ULK1(Ser555) between myotubes overexpressing AMPD3 versus GFP. After a 1 h recovery [AMP], AMP:ATP ratio, and [aspartic acid] were no different than vehicle treated, demonstrating recovery of energetics and cell viability. Long-term treatment with DNP significantly increased PGC-1α promotor activity (1.4-fold, $p<0.001$) compared to vehicle groups, while 5 days of AMPD3 overexpression significantly decreased PGC-1α promotor activity (1.3-fold, $p<0.005$) compared to GFP. Long-term DNP treatment increased the percentage of pixels positive for green florescence ($p<0.05$), however, myotubes overexpressing AMPD3 had significantly less than controls ($p<0.01$). **Conclusions:** Since activation of AMPK and PGC-1α are critical for increasing mitochondrial biogenesis, our results suggest that overexpression of AMPD3, such as occurs during muscle atrophy, is an important contributor to reductions in mitochondrial content.

AMP Deaminase 3 overexpression regulates cellular energetics and signaling for PGC-1α activation.

A Thesis

Presented to the Faculty of the Department of Kinesiology

East Carolina University

In Partial Fulfillment of the Requirements for the Degree

Master of Science in Kinesiology

Exercise Physiology Concentration

by

Spencer Miller

May, 2017

AMP Deaminase 3 overexpression regulates cellular energetics and signaling for PGC-1α activation.

by

Spencer Miller

APPROVED BY:

DIRECTOR OF THESIS: _____
Jeffrey J. Brault, Ph.D.

COMMITTEE MEMBER: _____
Carol A. Witczak, Ph.D.

COMMITTEE MEMBER: _____
Katsuhiko Funai, Ph.D.

COMMITTEE MEMBER: _____
Espen E. Spangenburg, Ph.D.

CHAIR OF THE DEPARTMENT
OF KINESIOLOGY: _____
Stacey R. Altman, J.D.

DEAN OF THE
GRADUATE SCHOOL: _____
Paul J. Gemperline, Ph.D.

TABLE OF CONTENTS

LIST OF FIGURES

CHAPTER 2

CHAPTER 4

Chapter 1: Introduction

In skeletal muscle, chronic increases in protein degradation result in substantial decreases in muscle mass, strength, and endurance in a process referred to as muscle atrophy. Muscle atrophy is a degenerative condition that can occur progressively with aging[1,2], rapidly with complete disuse or starvation[3–5], and pathologically with diseases such as cancer, diabetes, heart failure, and chronic kidney disease[6–9]. The onset of muscle atrophy during these conditions is a significant contributor to disability and mortality[10–12].

In addition to decreases in contractile proteins, muscles undergoing atrophy have decreased mitochondrial content[4,6,13] and cellular energetics[3,13–16], which is defined by decreases in the concentrations of high-energy phosphates: ATP or PCr, and increases in their degradation products: ADP, AMP, creatine, and P_i. Together, these result in muscles with diminished oxidative capacity, endurance, and force production[11,17,18]. These negative consequences of muscle atrophy and impairments in muscle function ultimately combine to decrease the individual's exercise capacity, which is also a powerful predictor of mortality[11,19]. Furthermore, exercise and muscle contractions during daily activities are critical for maintaining muscle mass, and the implementation of exercise interventions during disease can significantly improve clinical outcome[2,20–22]. Therefore, investigating the cellular mechanisms that contribute to decreased mitochondrial content is necessary for the identification of drug targets or therapeutic strategies that can preserve mitochondria and muscle function. In turn, this will help to maintain exercise capacity, ability to perform activities of daily living, and delay mortality in patients experiencing muscle atrophy.

Mitochondrial content is largely dependent on the balance between mitochondrial biogenesis, fusion/fission, and degradation[23,24]. Cellular mechanisms that signal for

mitochondrial biogenesis are activated in response to decreased cellular energetics[25,26]. In particular, increases in [AMP] have been shown to increase phosphorylation of AMP-activated protein kinase (AMPK), which in turn increases activation and expression of PGC-1α, ultimately resulting in mitochondrial biogenesis[26–29]. Muscles from several different atrophy models have decreased energetics[3,13–16], however, despite this, PGC-1α expression is decreased during atrophy[30–32]. Interestingly, chemical activation of AMPK via AICAR (an AMP mimetic) is sufficient to increase PGC-1α expression and preserve mitochondrial proteins during denervation induced atrophy[30]. This suggests that during atrophy AMPK is not activated and a possible explanation is that [AMP] is not increased due to increased enzyme activity of AMP Deaminase 3 (AMPD3).

Skeletal muscles from several different models of muscle atrophy have significantly upregulated AMPD3 expression, evident by a 5-100-fold increase in mRNA content, 3-fold increase in protein content, and a 34% increase in enzyme activity[31,33]. AMPD catalyzes the deamination of AMP to IMP with the release of ammonia as a byproduct ($AMP \rightarrow IMP + NH_3$)[34]. Therefore, increased activity of AMPD3 could potentially regulates mitochondrial content in skeletal muscle by decreasing [AMP], phosphorylation of AMPK, PGC-1α expression, and mitochondrial biogenesis. However, the effect of AMPD3 overexpression on these different markers of mitochondrial biogenesis is unknown.

Using C2C12 myotubes as a model of skeletal muscle, we sought to determine whether overexpression of AMPD3 was sufficient to attenuate increases in [AMP], phosphorylation of AMPK(Thr172), PGC-1α promotor region activity, and mitochondrial content caused by increased energy demand. As a model of energy, demand we used chemical treatment with the mitochondrial uncoupler 2,4 dinitrophenol (DNP), which allows protons to leak across the

mitochondrial inner membrane and decreases oxidative phosphorylation efficiency. We hypothesize that AMPD3 overexpression will attenuate DNP-induced increases in [AMP], phosphorylation of AMPK(Thr172), and PGC-1α promotor region activity. This will decrease activation of mitochondrial biogenesis and result in reduced mitochondrial content.

Chapter 2: Literature Review

Skeletal Muscle Atrophy

Muscle atrophy is characterized by smaller muscle fibers and fewer mitochondria, resulting in substantial loss of muscle mass, strength, and endurance [17,18,35]. Whether a muscle undergoes hypertrophy or atrophy is dependent on the balance between protein synthesis versus protein degradation. In skeletal muscle, signaling for protein synthesis is mediated through the phosphoinositide 3-kinase (PI3K)-Akt-mechanistic target of rapamycin (mTOR) pathway [36,37]. On the other hand, protein degradation is largely regulated by the transcription factor forkhead box protein O (FOXO), which controls the expression of several atrophy related genes [31,38,39]. Besides the FOXO family (FOXO1 & FOXO3), other transcription factors such as, SMAD2, SMAD3, NF-κB, along with glucocorticoids are known to regulate protein degradation [40–42].

There are two dominant cellular mechanisms involved in protein degradation: the autophagy-lysosome and the ubiquitin-proteasome systems [43,44]. Protein degradation by the ubiquitin-proteasome system involves the attachment of a polyubiquitin chain to targeted proteins by E3 ligases [45]. After being tagged with a polyubiquitin chain the proteins are unfolded and degraded by the proteasome complex [43]. Protein degradation by the autophagy-lysosome system involves the expansion of an autophagosome around proteins and organelles which then merge with the acidic lysosome to degrade proteins [44]. During atrophy the genes encoding for many components and regulators of these proteolytic mechanisms (ubiquitin ligases, proteasome subunits, autophagy mediating proteins) are significantly increased [31,36]. Protein degradation, especially the ubiquitin-proteasome system, is highly dependent on energy in the form of ATP [45–47]. Both ubiquitination of proteins and the unfolding/degradation of proteins by the proteasome require ATP. Furthermore, decreasing ATP concentration has been shown to slow ubiquitin-

proteasome mediated degradation [45,46], demonstrating the importance of cellular energetics on the control of overall protein content.

Mitochondrial content is decreased during atrophy

Atrophic muscles have decreased mitochondrial content and a depressed energy state (decreased [ATP] and/or increases in [ADP], [P_i]), which results in muscles with decreased specific force (force normalized to cross sectional area) and endurance [3,15–18,48]. This has clinical relevance considering low oxidative capacity is associated with increased risk of cardiovascular disease and mortality [49,50], as well as, the development of insulin resistance and type 2 diabetes [6,51,52].

Atrophy of myofibers and decreases in mitochondrial content occur during several common pathologies, including cancer [17,53,54], diabetes [6,55], and renal failure [7,48,56]. During cancer, 50-80% of patients can experience cachexia (chronic inflammation caused by pathology that causes muscle wasting), and almost 80% of those patients experiencing cachexia will die within 1 year of diagnosis [9,21,54]. These cancer cachectic muscles have impaired metabolic function and abnormal mitochondria[13]. Patients with type 2 diabetes mellitus experience muscle atrophy [6,55] along with reductions in PGC-1α and mRNA for oxidative phosphorylation proteins[31,57], resulting in decreased oxidative capacity and weaker muscles [58]. Patients with renal failure also experience substantial losses of muscle mass along with decreased mitochondrial and PGC-1α content [48,59].

Taken together, these studies show that muscle atrophy and decreased mitochondrial content are a consequence of disuse (denervation) and numerous chronic diseases (cancer, diabetes, renal failure). As a result, the oxidative capacity and endurance of skeletal muscle is decreased.

Regulation of Mitochondrial Biogenesis

Skeletal muscle is a dynamic tissue capable of changing its contractile properties and substrate utilization in response to various mechanical stimuli and metabolic demands. During repeated muscle contractions (i.e. physical activity/exercise) there is an increase in skeletal muscle ATP hydrolysis leading to increases in ADP, AMP, and P_i[34,60]. This increase in metabolic demand can be sensed through increases in intracellular [AMP], Ca^{2+}, and [NAD+]/[NADH] by several enzymes such as AMP activated protein kinase (AMPK), calcium/calmodulin-dependent protein kinase (CaMK), and silent mating-type information regulation 2 homolog 1 (SIRT1) [26,61–63] These enzymes respond to the decrease in energetics by activating the highly effective activator of mitochondrial biogenesis, PGC-1α (Figure 1) [29,63,64]

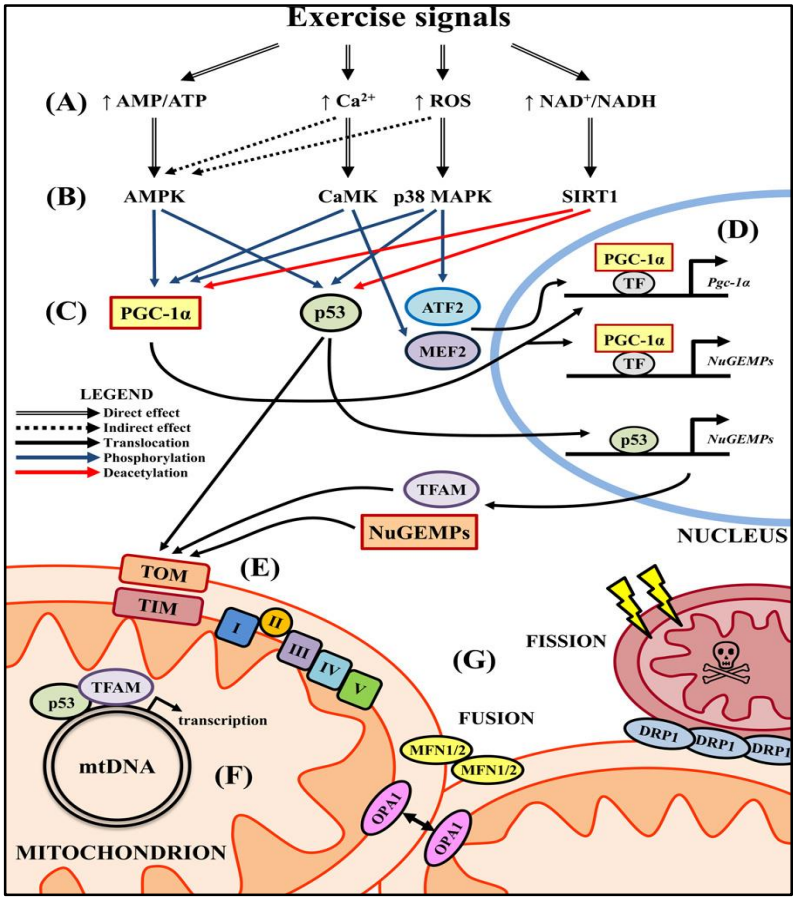

Figure 1. A) Muscle contractile activity alters the concentration of several metabolites and molecules involved in initiating mitochondrial biogenesis, including increasing the ratios of AMP/ATP and NAD+/NADH, as well as cytosolic calcium. These changes enhance the activity of a number of kinases (B), including AMPK, CaMK, and the deacetylase SIRT1. (C) These proteins increase the activation and expression of the transcriptional co-activator PGC-1*α*, which increases mitochondrial biogenesis by enhancing transcription of mitochondrial proteins.

(Hood et al., 2016).

AMPK regulation of mitochondrial biogenesis

When the rate of ATP hydrolysis exceeds the rate of ATP re-synthesis, such as that occurs during repeated muscle contractions or hypoxia, intracellular [ADP] increases. Furthermore, [AMP] also increases because of the near-equilibrium adenylate kinase (AK) reaction (ADP+ADP ↔ ATP+AMP) [65]. The increase in [AMP] and decrease in [ATP] activates the important cellular "energy sensor" AMP-activated protein kinase (AMPK)[28]. AMPK is a heterotrimeric Ser/Thr kinase composed of one catalytic (α) and two regulatory subunits (β,γ) . Activation of AMPK is enhanced upon the binding of its γ subunit by AMP, which increases the catalytic activity of the molecule and enhances phosphorylation of its α subunit Thr^{172} residue [28]. Several *in vivo* studies have investigated the effect of allosteric activation of AMPK on mitochondrial content [25,26,66]. Winder et al. subcutaneously injected rats with AICAR (when phosphorylated functions as an AMP mimetic and activates AMPK) and observed an increase in AMPK activity, along with an increase in cytochrome C and δ-aminolevulinate (ALA) synthase (ALA is mitochondrial matrix enzyme required for biosynthesis of heme, which is essential for electron transfer) in the quadriceps and soleus muscles. These muscles also exhibit a significant increase in citrate synthase, malate dehydrogenase, and succinate dehydrogenase (common markers of mitochondrial content). A similar study by Bergeron et al. used β-guanadinoproprionic acid (β-GPA) (a creatine homolog) to activate AMPK[25]. β-GPA works by competing for the transport of creatine, decreasing intracellular creatine content, inhibiting creatine kinase reaction, and therefore, reducing the energy buffering capacity of the muscle. In rats fed a diet supplemented with β-GPA, there is >85% reduction in muscle phosphocreatine and a ~40-50% reduction in ATP. After a 9 week diet (45% fat, 1% β-GPA) rats fed with β-GPA had a 42-70% increase in AMPK activity in white gastrocnemius and quadriceps muscles

compared to controls. Furthermore, there was a ~75% increase in ALA synthase mRNA and a significant increase in Cytochrome C content compared to controls. In addition to the evidence of increased mitochondrial content, Narkar et al. found that chronically activating AMPK via 4 weeks of oral AICAR treatment increased running endurance by 44% compared to controls [66].

In contrast to experimental activation of AMPK, others have generated muscle-specific null mice for AMPK β1 and β2 subunits (β1β2M-KO) to investigate the loss of AMPK activity in skeletal muscle metabolism[67]. Muscles of these mice have significant decreases in mitochondrial content and function as evident by ~30% decrease in cytochrome c oxidase activity, ~47% decrease in succinate dehydrogenase (SDH) activity, and ~56% in mitochondrial DNA copy number. Taken together these studies demonstrate that activation of AMPK is an important and potent regulator of mitochondrial content and function.

CaMK regulation of mitochondrial biogenesis

A hallmark of muscle contractions is an increase in intracellular Ca^{2+} ions. Because of its critical role in muscle contraction, researchers were led to investigate the effect of Ca^{2+} levels on mitochondrial biogenesis [62,63,68,69]. Increasing intracellular Ca^{2+} *in vitro* via treatment with Ca^{2+} ionophores or caffeine (stimulates release of Ca^{2+} from sarcoplasmic reticulum) induces the expression of mitochondrial genes[68,69]. The increase in intracellular Ca^{2+} activates calcium dependent enzymes such calcineurin and calcium/calmodulin-dependent protein kinase (CaMK), which are known to signal expression of oxidative fiber-type genes [63]. Therefore, it seemed logical that CaMK was involved in the signaling of mitochondrial biogenesis, and Wu et al. developed transgenic mice that expressed a muscle-specific constitutively active form of CaMK isoform IV in hopes to elucidate the specific mechanism[63]. The CaMK mice had substantially higher amounts of type I oxidative fibers and mitochondrial content compared to wild-type.

Microarrays of gene expression found increases in mRNA of several mitochondrial proteins such as NADH dehydrogenase, cytochrome B, cytochrome C, and Carnitine Palmitoyltransferase-1 (CPT-1) compared to wild-type. Furthermore, the transgenic mice had increased expression of PGC-1α and the proximal promotor region of the PGC-1α gene was activated 4-fold higher in CaMKIV active C2C12 myotubes. These studies demonstrate that contractile activity associated increases in intracellular Ca^{2+} signals for mitochondrial biogenesis through a CaMK-PGC-1 transcriptional mechanism.

SIRT1 regulation of mitochondrial biogenesis

Another mechanism by which contractile activity signals for mitochondrial biogenesis is through activation of silent mating-type information regulation 2 homolog 1 (SIRT1) [61,70,71]. Sirtuins are deacetylase enzymes that are activated by increases in intracellular NAD+/NADH concentrations. SIRT1 has been shown to regulate mitochondrial biogenesis through deacetylation of downstream targets such as PGC-1α and HIF-1α[64]. Interestingly, SIRT1 activity is also regulated by AMPK through AMPK mediated increases in [NAD+] [61,64,72].

PGC-1α regulation of mitochondrial biogenesis

AMPK, CaMK, and SIRT1 regulate mitochondrial content through activation of the transcriptional coactivator, peroxisome proliferator-activated receptor γ co-activator-1α (PGC-1α)[23]. PGC-1α is widely considered a potent regulator of mitochondrial biogenesis as it is sufficient to induce mitochondrial biogenesis and is activated by several cellular signaling pathways all related to contractile activity and increased metabolic demand [30,73,74]. PGC-1α exists in the cytosol and once activated translocates to the nucleus where it activates transcription of its own mRNA, as well as, numerous transcription factors including nuclear respiratory factors (NRF 1-2), PPAR family, and mitochondrial transcription factor A (Tfam)[27,75]. These

transcription factors then increase the expression of genes involved in mitochondrial biogenesis such as NuGEMPs (mitochondrial proteins encoded in nuclear DNA), mtDNA (mitochondrial proteins encoded in mitochondrial DNA), and numerous oxidative metabolism genes..

PGC-1α was first discovered as a coactivator of PPARγ in studies examining differential gene expression in brown adipose tissue during response to cold-induced adaptive thermogenesis[76].Transgenic mice that overexpress PGC-1α in skeletal muscle demonstrate greater voluntary exercise activity and significantly higher aerobic capacities, as determined by peak VO_2 consumption, compared to wild-type mice [75]. Calvo et al. also measured mitochondrial protein content and found that PGC-1α transgenic mice had expansive increases in proteins involved in fatty acid oxidation and oxidative phosphorylation. Enzymatic activity of citrate synthase was higher in both gastrocnemius and tibialis anterior muscles, signifying functional increases of mitochondria.

Similarly, PGC-1α knockout mice have reduced mitochondrial content, function, and mitochondrial gene expression [27,77]. Handschin et al. generated muscle-specific PGC-1α knockout mice and then measured markers of mitochondria content and function. There was a reduction of mRNA for several mitochondrial proteins and enzymes. The mice had decreased voluntary exercise compared to wild-type controls as well as a 28% decrease in total time till exhaustion on a treadmill indicating decreased muscle endurance and aerobic capacity. Taken together, these studies demonstrate why PGC-1α is considered a master regulator of mitochondrial biogenesis.

Regulation of Mitochondrial Degradation

Maintaining the functional capacity of mitochondria requires the coordinated process of selectively separating and degrading damaged mitochondria via fission and mitophagy

(autophagy of mitochondria) and incorporating newly synthesized proteins back into the mitochondrial matrix [24]. Mitophagy is critical to maintain mitochondria capable of preserving energy homeostasis and healthy skeletal muscle [24,78].

In congruence with their regulation of mitochondrial biogenesis, AMPK and SIRT1 also function to regulate mitophagy. Activation of AMPK has been shown to induce mitophagy by direct phosphorylation of unc-51-like kinase 1 (ULK1) on serine 317, 555, and 777 residues [79,80]. Phosphorylation of ULK1 is the first reaction in a signaling cascade leading to the recruitment, expansion, and formation of the autophagosome. Activated SIRT1 is shown to contribute to mitophagy through deacetylation of autophagy-related gene 7 (Atg7) which is critical for autophagosome membrane expansion[81]. The effect of AMPD3 overexpression on AMPK and SIRT1 mediated autophagy is unknown.

The role of AMP Deaminase

During high energy demanding conditions the hydrolysis of ATP can increase 100 fold[60]. When ATP hydrolysis outpaces synthesis, cellular ATP content declines and ADP and AMP accumulate. The increase in [ADP] and [AMP] activate the enzymatic reactions of adenylate kinase ($ADP+ADP \leftrightarrow ATP+AMP$) and AMP deaminase ($AMP \rightarrow IMP+NH_3$). Together, these reactions serve to limit the accumulation of [ADP] and [AMP] in order to maintain the ATP: ADP: AMP ratios, and preserve the energy state of the cell [65]. Along with maintaining the relative ratios of adenine nucleotides, AMPD catalyzes the entry reaction of the purine nucleotide cycle (Figure 2). The purine nucleotide cycle is a multistep process that generates citric acid cycle intermediates while catalyzing the reamination of IMP [82,83]. Activity of the purine nucleotide cycle is dependent on AMPD activity and genetic mutations that result in loss

of AMPD1 expression in skeletal muscle have been suggested to impair muscle function through reduced purine nucleotide cycle activity[83,84].

AMP Deaminase increased during atrophy

Using microarray hybridization of cDNA, differential mRNA expression for genes involved in muscle atrophy were quantified [31,32,85]. These studies mapped a common transcriptional profile for most if not all types of muscle atrophy (denervation, starvation, cancer-cachexia, diabetes, renal failure) and allowed for the identification of novel transcriptional changes that occur during rapid muscle loss. Along with predictable genes involved in protein synthesis and degradation, genes involved in energy metabolism were also identified. In general, the mRNA for genes involved in ATP synthesis (including PGC-1α), glycolysis, and ketone metabolism were significantly reduced. Conversely, an increase in mRNA expression was measured for genes encoding glutamine synthase, IMP dehydrogenase 2, and AMP deaminase isoform 3. Surprisingly, AMPD3 had one of the largest increases in expression, being 5-100 fold increased depending on the atrophy condition. These findings are similar to an earlier *in vivo* study's findings that upon denervation induced atrophy, total AMPD activity increased by 34% and the protein content of AMPD3 increased three-fold [33]. Increased expression of AMPD3 is significant for mitochondrial biogenesis considering that AMPD would be expected to bind and/or degrade AMP, lower

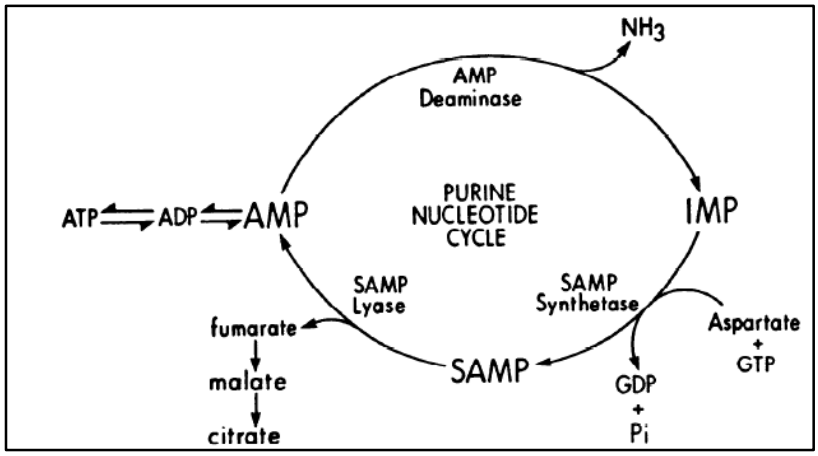

Figure 2. AMP Deaminase is the entry reaction into the purine nucleotide cycle. (Flanagan, et al. 1986)

intracellular [AMP], thus, inhibit activation of AMPK. The general role of AMPD3 during atrophy and its specific effects on mitochondrial content are unknown.

Specific Aims

Atrophic muscles from multiple conditions (denervation, diabetes, cancer cachexia, starvation, renal failure) have decreases in intracellular ATP and creatine phosphate levels [3,13–16]. Normally this would result in activation of several energy sensing molecules, most notably AMPK, which would in turn activate and increase PGC-1α content subsequently leading to increased mitochondrial biogenesis[23]. However, atrophic muscles have decreased PGC-1α and mitochondrial content despite having depressed energetics[31]. Chemical activation of AMPK during atrophy via AICAR resulted in increased PGC-1α and mitochondrial content[30] suggesting that atrophic muscles are still capable of responding to AMPK but the main signal, [AMP], is undetected.

We hypothesize that increased AMPD3 expression limits the accumulation of AMP within the cell and attenuates signaling for mitochondrial biogenesis. Therefore the purpose of this study was to determine the effect of overexpressing AMPD3 on adenine nucleotides, AMPK phosphorylation, and PGC-1α expression *in vitro.*

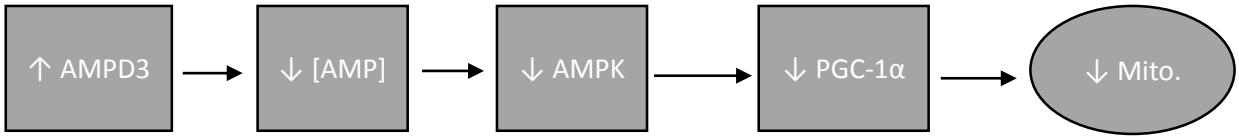

Figure 3. Proposed mechanism of AMPD3 regulation of mitochondrial content.

Specific Aims:

1) To determine if AMPD3 overexpression is sufficient to decrease [AMP] and phosphorylation AMPK(Thr172) in C2C12 myotubes both at rest and during a short-term energy demand.

2) To determine if AMPD3 overexpression decreases PGC-1α promotor activity in C2C12 myotubes

Chapter 3: Methods

Experimental Design

In order to test our hypothesis that AMPD3 attenuates increases in [AMP] and phosphorylation of AMPK(Thr172), we overexpressed AMPD3 in C2C12 myotubes for 24 hours using adenovirus. At hour 23, we treated myotubes with of 0.6 mM 2,4 dinitrophenol (DNP) for 1 hour, to reduce cellular energetics (↓[ATP], ↑[ADP], ↑[AMP]) and stimulate AMPK phosphorylation. We used this model to stimulate AMPK, compared to direct chemical activation, because we believe that increased AMPD activity is an upstream regulator of AMPK. Thus, directly activating AMPK using chemical activators (such as AICAR) would not increase [AMP] and bypass the AMPD reaction. Furthermore, nucleotides and proteins were collected immediately after treatment to determine changes in energetics and protein phosphorylation. Nucleotides were collected again at 1 hour post DNP treatment to ensure cell viability. To determine long-term effects of AMPD3 on PGC-1α expression we transfected myoblasts with a 2kb PGC-1α -Luciferase reporter, differentiated myotubes, and then chronically expressed AMPD3 (5days) and treated with continuous DNP (4days).

Cell Culture

C2C12 mouse myoblasts were grown on gelatin-coated 6-well plates in Dulbecco's modified Eagle's medium (DMEM) with 10% fetal bovine serum, penicillin (100 μg /mL), and streptomycin (100 μg/mL) until 75-90% confluent. Media was then switched to DMEM with 2% horse serum and penicillin/streptomycin to allow for differentiation into multi-nucleated myotubes. Four days after differentiation, myotubes were transduced with adenovirus encoding AMPD3-GFP or GFP (Vector Biolabs). Twenty-four hours after transduction myotubes were treated with 0.6 mM DNP or vehicle (methanol) added to differentiation media for 1 hour.

Nucleotides were collected on ice by PCA extraction immediately after. For recovery measurements, myotubes were washed twice with phosphate buffered saline (PBS), given fresh differentiation media, and then nucleotides were collected 1 hour after washing. For long-term treatment experiments, myotubes were differentiated and virus was transduced 24 hours later. Twenty-four hours after transduction myotubes were treated chronically with a 100 μM DNP dosage. Every 24 hours the media was exchanged with a fresh DNP+DMEM solution to ensure chronic uncoupling. To confirm virus transduction efficiency, GFP florescence was checked every 24 hours using florescent microscopy.

Western blot analysis

Proteins were extracted from cells in radio-immunoprecipitation (RIPA) buffer including protease inhibitors (Roche, complete) and quantified by BCA Assay (Pierce). Equal amounts of protein (7.3 μg/well) were separated by SDS-PAGE (10% polyacrylamide) then transferred to polyvinylidene difluoride (PVDF) membranes. Equal loading and transfer was confirmed by Ponceau S staining. Membranes were blocked for 1 hour at room temperature using a 5% BSA dissolved in TBS-T solution. Primary antibodies were purchased from ABCAM (AMPD3; ab118230), Cell Signaling (AMPKα #5831; pAMPK thr172 #2531, ULK1 #DH85, pULK1 ser555 #DIH4), and Millipore (pACC ser79 Lot #JC1938937). Antibodies were diluted in a solution of tris-buffered saline 0.1% tween-20 (TBS-T) with 2% bovine serum albumin. Membranes were incubated in primary antibody overnight at 4°C. Secondary antibodies conjugated to horseradish peroxidase (Cell Signaling #7074, ThermoFisher #31444) were detected with Western Chemiluminesence HRP Substrate (EMD Millipore). Band intensities were captured using a Bio-Rad Chemi Doc XRS imager and analyzed using Image Lab Software

(Bio-Rad). Approximate molecular weights of protein were calculated relative to PageRuler Plus protein ladder (ThermoFisher).

Nucleotide and Aspartic acid Measurements

C2C12 myotubes were washed twice with ice cold PBS, and nucleotides were extracted in ice cold 0.5 N PCA + 5mM EDTA and stored in Eppendorf tubes. After sonication, precipitated proteins were pelleted by centrifugation (10,000 rpm for 10 minutes at 4°C) and the supernatant removed. Supernatants were neutralized by the addition of ice cold 1 N KOH and centrifugation at 4°C to remove potassium-perchlorate salt. Supernatants were stored at -80°C until analysis. Protein pellets were re-suspended in 0.2 N NaOH for protein estimation by BCA Assay (Pierce).

Adenine nucleotide concentrations (ATP, ADP, AMP) and degradation products (IMP, adenine, and inosine) are determined by ultra-performance liquid chromatography (UPLC) using a Waters Acquity UPLC H-Class system and an Acquity UPLC HSS T3 1.8 μm, 2.1 mm X 150 mm column (Waters) as done previously [86].

Aspartic acid was measured by UPLC using the AccQ-Tag Ultra Derivitization kit (Waters). PCA extracts were diluted in a borate buffer and then combined with AccQ tag reagent. After incubation at 55°C, the amine group of aspartic acid is labeled with 6-aminoquinolyl-N-hydroxysuccinimidyl carbamate (AQC), which makes this amino acid easily detectable using UV absorbance.

Reporter activity

To measure PGC-1α promotor activity, myoblasts were transfected with plasmids encoding a 2kb PGC-1α promotor-firefly luciferase (addgene, plasmid #8887, as described by [27]) and HSV-thymidine kinase promotor- renilla luciferase (Promega). Twenty-four hours after

transfection myoblasts were switched to differentiation media. To determine luciferase activity we followed the Promega Dual-Luciferase Reporter Assay protocol. Briefly, myotubes are washed twice with PBS, and then passive lysis buffer is added. After a 15-30 minute incubation at room temperature, cell lysates are collected. Firefly and renilla luciferase activity are measured separately as instructed by Promega. Luciferase activity is normalized to renilla values.

Microscopy Imaging

To stain for mitochondria area and nuclei, myotubes were treated with 100 nM of MitoTracker Green FM (Life Technologies) and 2 µg/ml Hoescht 33343 (nuclei) dissolved in differentiation media. After 30 minutes of incubation at 37°C, growth media was switched to FlouroBrite DMEM and fluorescent images were captured using filters typically used for GFP and DAPI. Mitochondria area was quantified using ImageJ software. After subtracting the background, images were converted to binary and the percent of positive pixels was quantified.

Statistics

Significant differences between DNP concentrations were determined by a one way ANOVA and Tukey's post hoc analysis test with $p<0.05$. Significant differences between the 4 experimental groups (Vehicle+GFP, Vehicle+AMPD3, DNP+GFP, DNP+AMPD3) was determined using a 2x2 ANOVA with $p<0.05$. PGC-1α reporter data was analyzed using an unpaired two-tailed t-test between experimental groups with significance set at $p<0.05$. Data was analyzed using GraphPad Prism 7.0 software. All samples sizes were 4-6 replicates per condition.

Chapter 4: Results

Effects of short-term AMPD3 overexpression on adenine nucleotide metabolism and AMPK.

In order to test the effect of AMPD3 overexpression on the activation of AMPK, we needed establish a condition of energy demand that would be sufficient to decrease cellular energetics and specifically cause increases in the concentration of AMP. To do this we treated myotubes with the mitochondrial uncoupler 2,4 dinitrophenol (DNP). To determine an appropriate dosage of DNP, we treated C2C12 myotubes with 0, 0.4, 0.6, 0.8, and 1 mM DNP, and collected samples 1 hour later for measurement of nucleotides (Figure 1). Increasing DNP concentrations resulted in a progressive decrease in [ATP], ranging from 45.0 µmol/g protein in vehicle (methanol) treated to 16.8 µmol/g at 1 mM DNP (Fig. 1a). As expected, [ADP] increased with DNP, peaking at 8.3 µmol/g with 0.6 mM DNP, but interestingly decreased to 6.5 and 5.3 µmol/g with 0.8 and 1 mM DNP (Fig. 1b). [AMP] doubled from 0.34 µmol/g in vehicle to 0.68 µmol/g at 0.4 mM, but then rose markedly with increasing DNP concentrations peaking at 7.8 µmol/g, a 23-fold increase versus vehicle (Fig. 1c). The decreases in [ATP] and increases in [AMP] subsequently resulted in a nearly 60-fold increase in the AMP:ATP ratio, from a value of 0.008 in vehicle to 0.46 in 1 mM DNP groups (Fig. 1d). Similar to [AMP], [IMP] rose with increasing concentrations of DNP, ranging from undetectable in vehicle to 4.7 µmol/g at 1 mM DNP (Fig. 1e). Total adenine nucleotides and IMP (AN+IMP) decreased linearly from 49.8 µmol/g in vehicle to 34.6 µmol/g at 1 mM DNP (Fig. 1f), which suggests that nucleotides (AMP and IMP) were further metabolized to nucleosides (adenosine or inosine). From these findings we concluded that 0.6 mM DNP would be most appropriate dose to test our hypothesis because it significantly increased [ADP] (1.8-fold), [AMP] (6-fold), and the AMP:ATP (9-fold) compared to vehicle groups. In contrast, 0.4 mM DNP did not produce significant increases in [AMP] or

the AMP:ATP ratio. Furthermore, 0.6 mM DNP resulted in modest reductions of AN+IMP from 49.8 in vehicles to 45.3 as opposed to larger decreases with 0.8 and 1 mM DNP.

After determining the optimal DNP dose, we then tested the effect of acutely overexpressing AMPD3 (24 hrs.) and treatment with or without DNP (1 hr.) on intercellular concentration of adenine nucleotides and IMP (Figure 2). To control for any effect of adenovirus transduction and general effects of protein overexpression, we transduced myotubes with an adenovirus overexpressing GFP. Furthermore, to control for any effect of the DNP solvent methanol, we treated vehicle groups with equal volumes of methanol. Therefore, we had four experimental groups: vehicle-GFP, vehicle-AMPD3, DNP-GFP, and DNP-AMPD3. After 24 hours of AMPD3 and 1 hour of DNP, veh-AMPD3 had significantly less (1.3-fold) [ATP] compared to veh-GFP, while DNP-AMPD3 had significantly less (1.5-fold) [ATP] compared to DNP-GFP. AMPD3 overexpression also resulted in significantly less [ADP] in both vehicle (1.4-fold) and DNP (2-fold) groups. As predicted DNP-AMPD3 had significantly less (6.3-fold) [AMP] compared to DNP-GFP. This was reflected by a significantly attenuated increase in the AMP:ATP, with DNP-GFP groups experiencing a 24-fold increase compared to veh-GFP, while DNP-AMPD3 experiencing only a 9-fold increase compared to veh-AMPD3. Veh-AMPD3 had 0.41 µmol/g [IMP] compared to undetectable for veh-GFP, signifying basal AMPD activity, and DNP-AMPD3 had significantly greater (2.9-fold) [IMP] compared to DNP-GFP. Veh-AMPD3 had significantly less (1.2-fold) AN+IMP compared veh-GFP, and similarly DNP-AMPD3 had significantly less (1.4-fold) compared to DNP-GFP.

These findings show that both AMPD3 and DNP can significantly decrease the total adenine nucleotide pool within the cell of which could have potentially lethal consequences. Therefore we next sought to determine whether nucleotide concentrations would return back to

steady-state levels after DNP. To test this we treated myotubes with 0.6 mM DNP for 1 hour, washed twice and switched to DNP free media, and then collected nucleotides at 1 hour post DNP treatment (Figure 3). DNP groups had significantly less [ATP] than vehicle groups, yet no differences existed between GFP and AMPD3 (Fig. 3a). DNP groups had significantly less [ADP] than vehicle groups, and DNP-GFP had significantly less (1.5-fold) [ADP] than DNP-AMPD3 (Fig. 3b). Notably [ADP] from DNP-GFP was 3-fold less than levels measured immediately after DNP treatment. No differences were measured in [AMP] between vehicle and DNP groups or AMPD3 and GFP (Fig 3c). However, similar to [ADP], [AMP] concentrations returned back to pre-DNP levels and this resulted in AMP:ATP ratio also returning back to previous values (Fig. 3d). This trend continued with [IMP] decreasing to pre-DNP levels and was significantly greater with AMPD3 in both vehicle (from undetectable) and DNP (10-fold) compared to GFP groups (Fig. 3e). DNP groups had significantly less AN+IMP than vehicle groups, yet no differences existed between AMPD3 and GFP groups (Fig. 3f). These results show that 1 hour after DNP treatment [ADP], [AMP], AMP:ATP, and [IMP] return back to steady-state levels, suggesting that the myotubes are still viable because they have begun the recovery process.

The deamination of AMP to IMP is catalyzed by AMPD and is the entry reaction for the purine nucleotide cycle. The purine nucleotide cycle is a multistep process that leads to the reamination of IMP to AMP with an amine group donated from aspartic acid (Figure 2 in lit. review). Therefore, aspartic acid concentrations can be used an indirect measure of purine nucleotide cycle activity. In the same samples that we collected for measurements of nucleotide content, we also measured aspartic acid concentration (Figure 4). After a 1 hour treatment with DNP aspartic acid was significantly greater in DNP groups (Fig. 4a). However, after a 1 hour

recovery period the concentration of aspartic acid in DNP treated myotubes had decreased significantly below levels of the vehicle treated myotubes (Fig. 4b). No differences were measured between GFP and AMPD3 at either time point. These findings suggest that during an energy demand purine nucleotide cycle is relatively inactive but after a short recovery period (1 hr.) activity resumes, presumably to increase reamination of IMP to AMP and maintain intracellular concentration of the adenine nucleotide pool.

We show that AMPD3 attenuates the increase in [AMP] during a cellular energy demand induced by DNP (Figure 2). Therefore, we next collected proteins under the same conditions to determine if the attenuated increase in [AMP] would decrease the phosphorylation of AMPK(Thr172), as well as, the phosphorylation of several AMPK downstream targets (Figure 5). As expected, DNP treatment significantly increased the amount of phosphorylated AMPK (pAMPK) and the ratio of phosphorylated AMPK to total AMPK (Fig. 5b & 5c). However, overexpression of AMPD3 limited the increase in pAMPK in both vehicle and DNP conditions, which together resulted in a significant main effect decrease compared to GFP groups. Importantly, we also confirmed that AMPD3 was overexpressed (Fig. 5d). DNP significantly increased the phosphorylation of downstream AMPK targets, unc-51-like kinase 1 (ULK1) and acetyl CoA carboxylase (ACC), however, no significant differences were detected between AMPD3 and GFP groups (Fig. 5f & 5g). The differences in pAMPK (Fig. 5b) along with the attenuated increase in the AMP:ATP ratio (Fig. 2d) indicate that AMPD3 overexpression can limit the intracellular signaling response to low energy conditions short term.

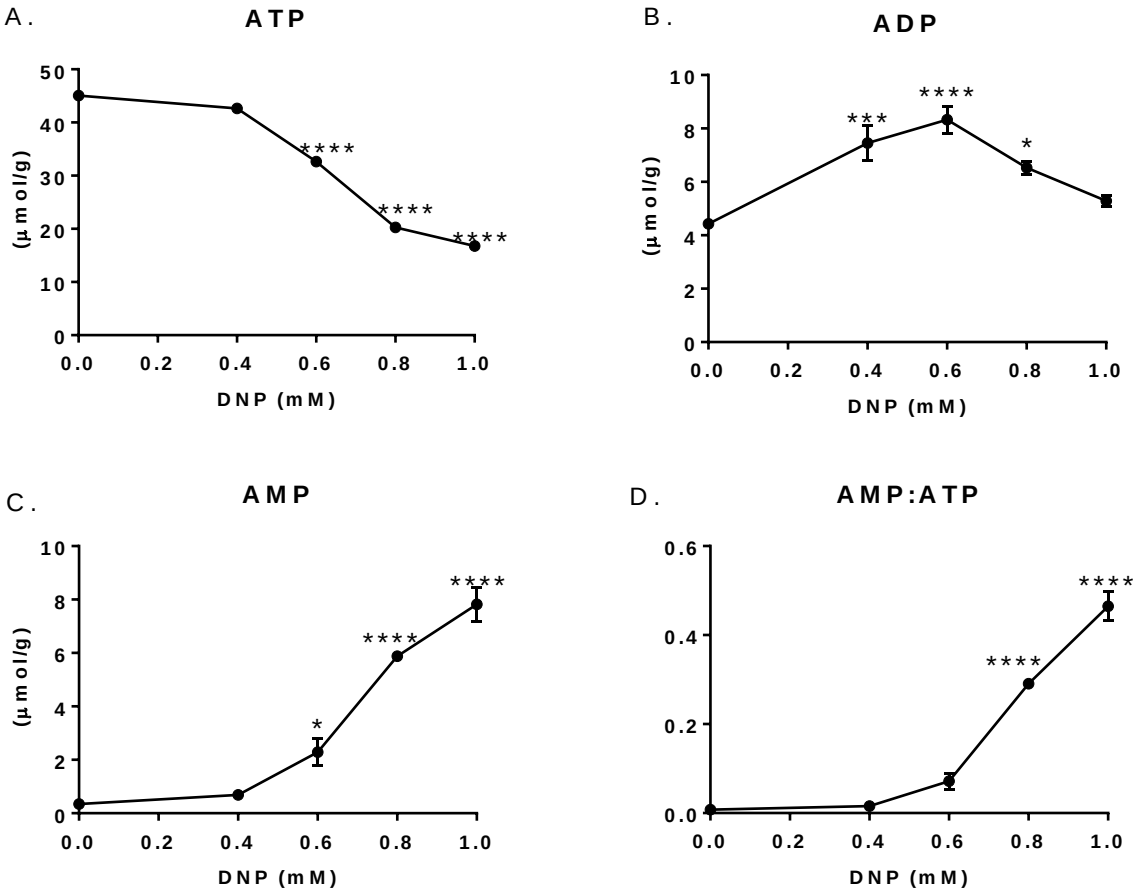

Figure 1. DNP decreases cellular energetics in a dose dependent fashion. C2C12 myotubes were treated with 0, 0.4, 0.6, 0.8, and 1 mM concentrations of 2,4 dinitrophenol (DNP) for 1 hour. Nucleotides were extracted immediately after treatment. A-C. Adenine nucleotide concentrations normalized to total protein content. D. The calculated ratio of AMP to ATP.
*= $p<0.05$, **= $p<0.005$, ***= $p<0.001$, ****= $p<0.0001$

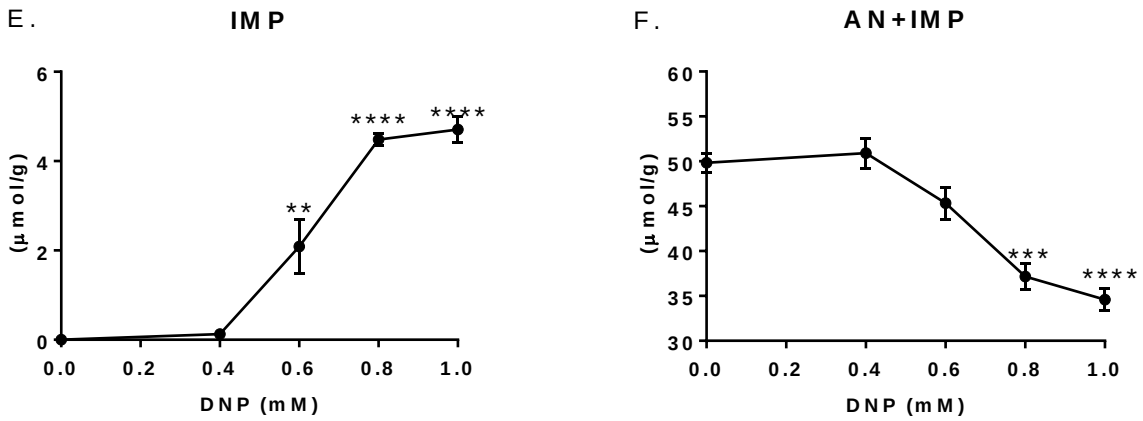

Figure 1. **DNP decreases cellular energetics in a dose dependent fashion**. C2C12 myotubes were treated with 0, 0.4, 0.6, 0.8, and 1 mM concentrations of 2,4 dinitrophenol (DNP) for 1 hour. Nucleotides were extracted immediately after treatment. E. IMP concentrations normalized to total protein. F. Total adenine nucleotides plus IMP (AN+IMP).
**= $p<0.005$, ***= $p<0.001$, ****= $p<0.0001$

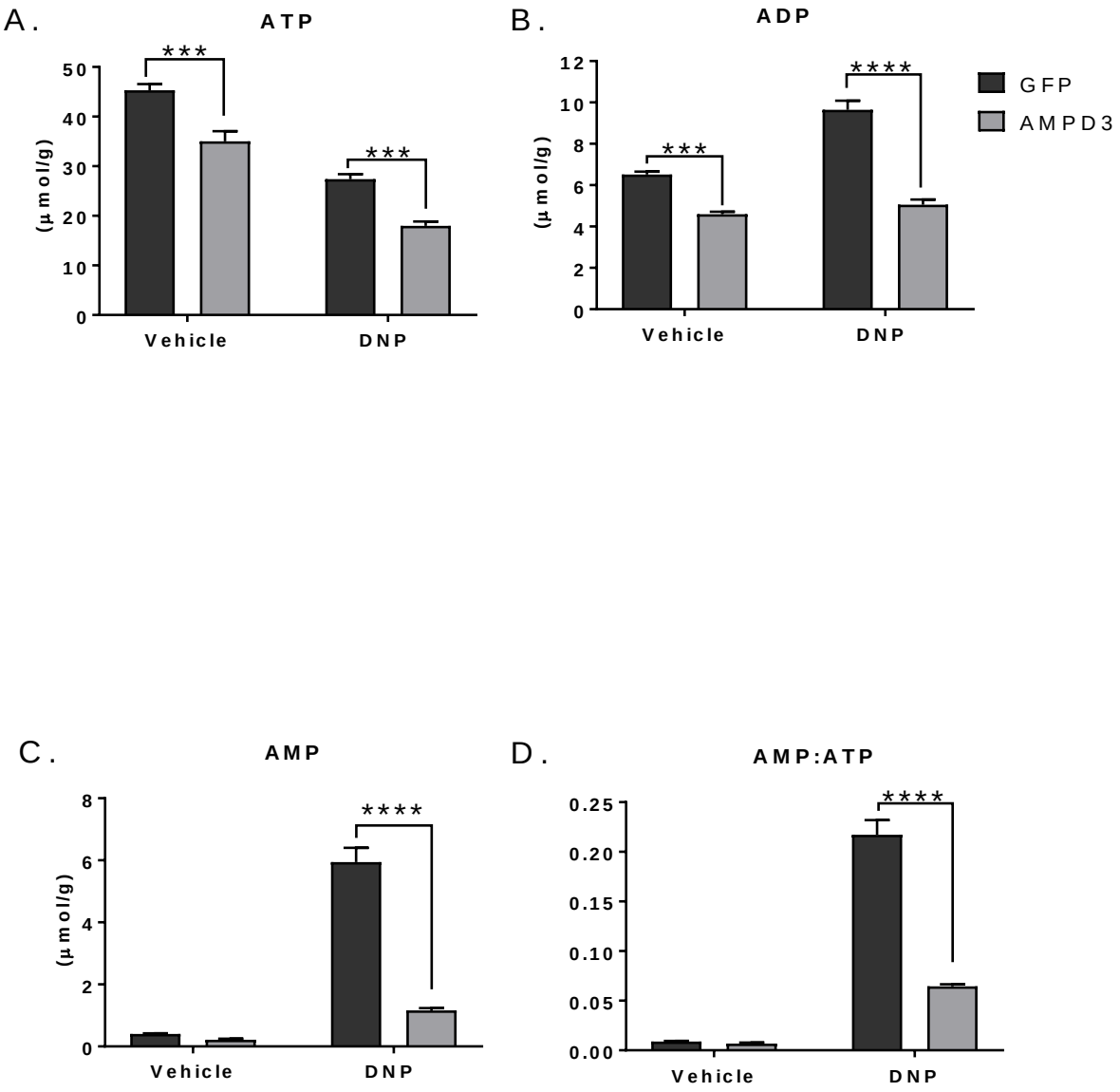

Figure 2. AMPD3 prevents increase in ADP and AMP during energy demand. C2C12 myotubes were transduced with adenovirus encoding either GFP or AMPD3 for 24 hours. At 23 hours post viral transduction myotubes were treated with 0.6 mM 2,4 dinitrophenol (DNP) or vehicle (methanol) for 1 hour. Nucleotides were extracted immediately after DNP treatment and measured by UPLC. A-C. Adenine nucleotide concentrations normalized to total protein content. D. The calculated ratio of AMP to ATP.
***= $p<0.001$, ****= $p<0.0001$

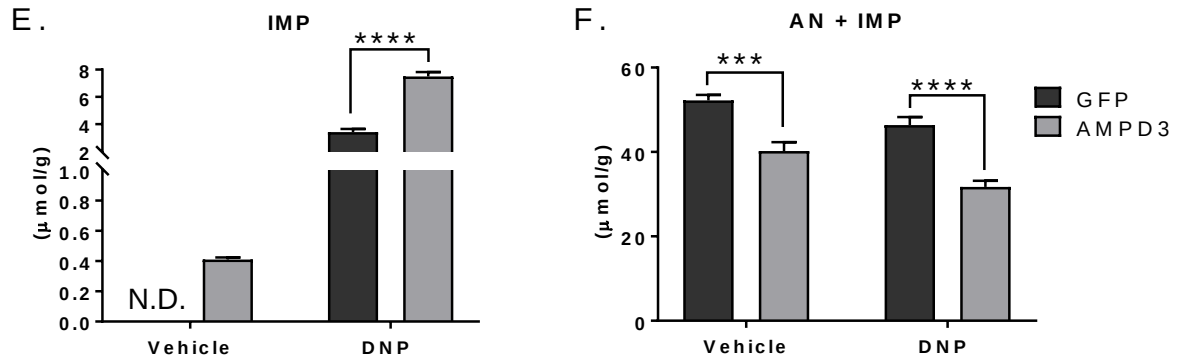

Figure 2. AMPD3 prevents increase in ADP and AMP during energy demand. C2C12 myotubes were transduced with adenovirus overexpressing either GFP or AMPD3 for 24 hours. At 23 hours post viral transduction myotubes were treated with 0.6 mM 2,4 dinitrophenol (DNP) or vehicle (methanol) for 1 hour. Nucleotides were extracted immediately after DNP treatment and measured by UPLC. E. IMP concentrations normalized to total protein content. F. Total adenine nucleotides with the addition of IMP (AN+IMP).
***= $p<0.001$, ****= $p<0.0001$, N.D.= none detected

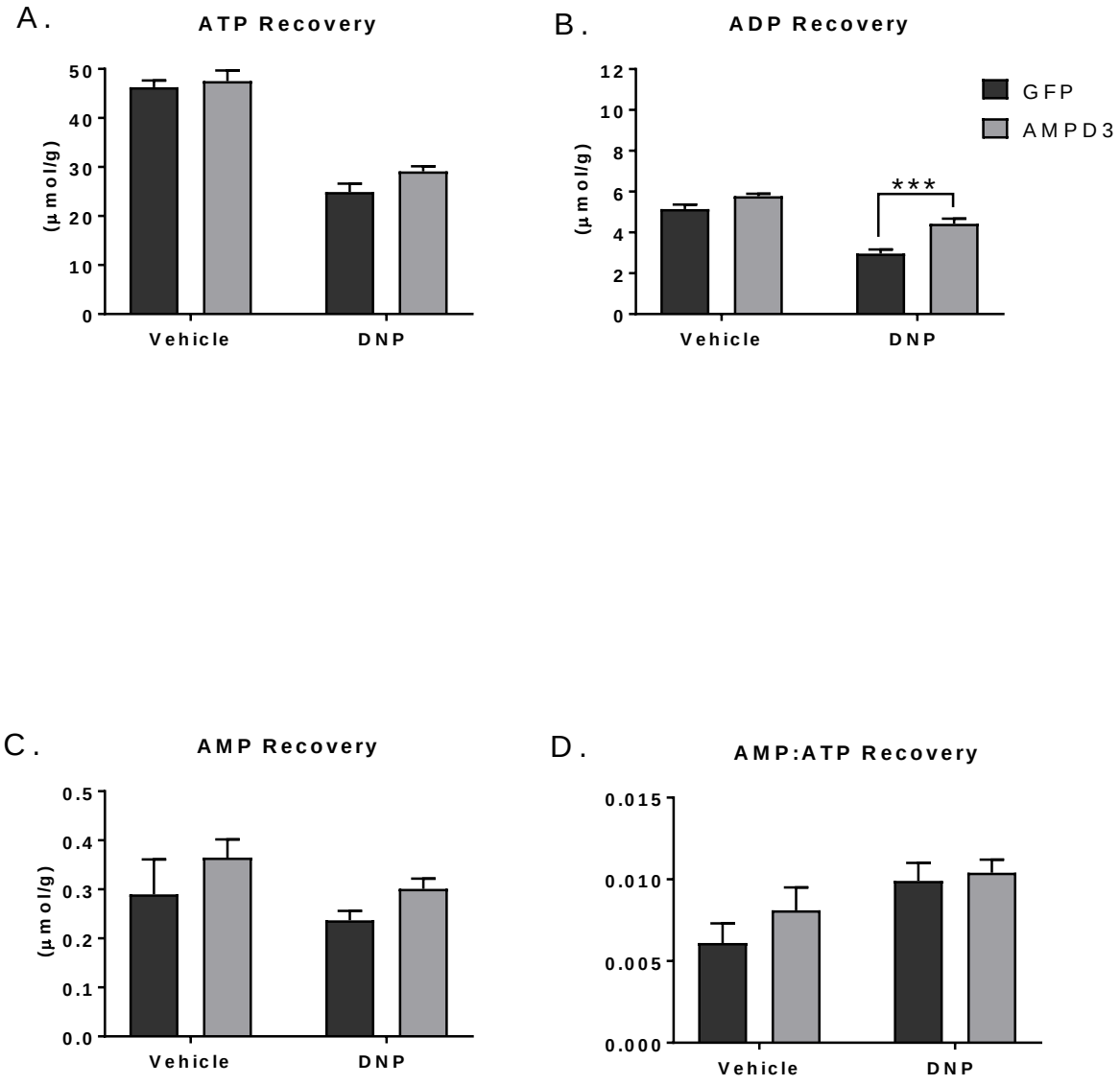

Figure 3. Cellular energetics recover after an acute bout of DNP. C2C12 myotubes were transduced with adenovirus encoding either GFP or AMPD3 for 24 hours. At 23 hours post viral transduction myotubes were treated with 0.6 mM 2,4 dinitrophenol (DNP) or vehicle (methanol) for 1 hour, and then allowed 1 hour of recovery before extraction. A-C. Adenine nucleotide concentrations normalized to total protein content D. The calculated ratio of AMP to ATP. ***= $p<0.001$

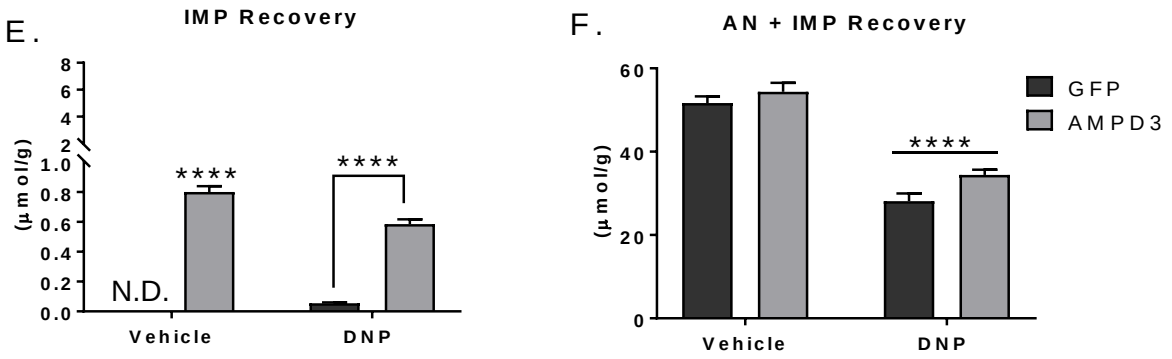

Figure 3. Cellular energetics recover after an acute bout of DNP. C2C12 myotubes were transduced with adenovirus encoding either GFP or AMPD3 for 24 hours. At 23 hours post viral transduction myotubes were treated with 0.6 mM 2,4 dinitrophenol (DNP) or vehicle (methanol) for 1 hour, and then allowed 1 hour of recovery before extraction. E. IMP concentration normalized to total protein content. F. Total adenine nucleotides with the addition of IMP (AN+IMP). ***= $p<0.001$, ****= $p<0.0001$, N.D. = none detected

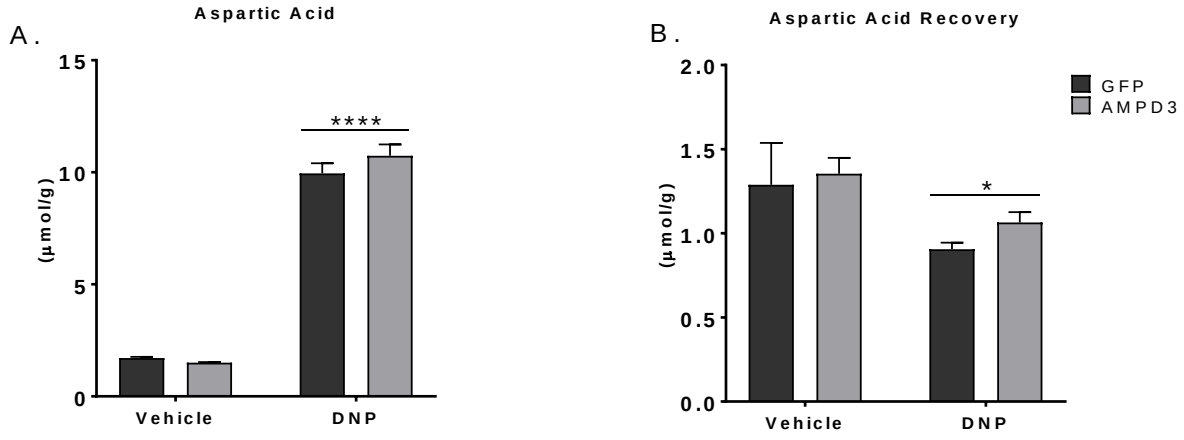

Figure 4. Aspartic acid, a substrate of the purine nucleotide cycle, increases during energy demand. C2C12 myotubes were transduced with adenovirus encoding either GFP or AMPD3 for 24 hours, treated with 0.6 mM 2,4 dinitrophenol (DNP) or vehicle (methanol) for 1 hour, and then allowed 1 hour of recovery before extraction. A. Aspartic acid concentration immediately after DNP treatment. B. Aspartic acid concentrations 1 hour after DNP treatment.
*= $p<0.01$, ****= $p<0.001$

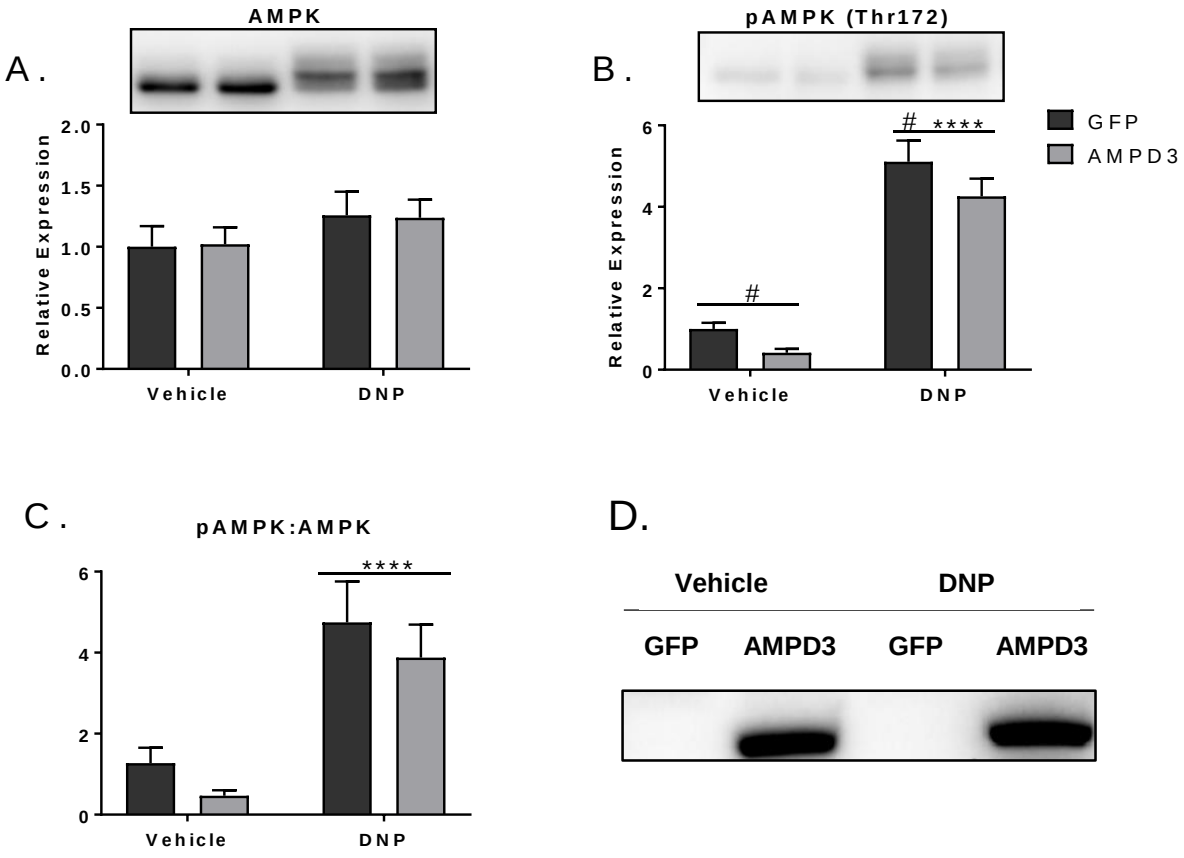

Figure 5. AMPD3 overexpression limits the phosphorylation of AMPK. C2C12 myotubes were transduced with adenovirus encoding either GFP or AMPD3 for 24 hours and treated with 0.6 mM 2,4 dinitrophenol (DNP) or vehicle (methanol) for 1 hour. Proteins were extracted and expression levels were measured by Western Blot. A. Protein expression levels of AMPK. B. Protein expression levels of phosphorylated AMPK (Thr172). C. Calculated ratio of phosphorylated AMPK to total AMPK. D. Representative western blot for AMPD3. # = main effect of AMPD3 p=0.05, ****= p<0.0001

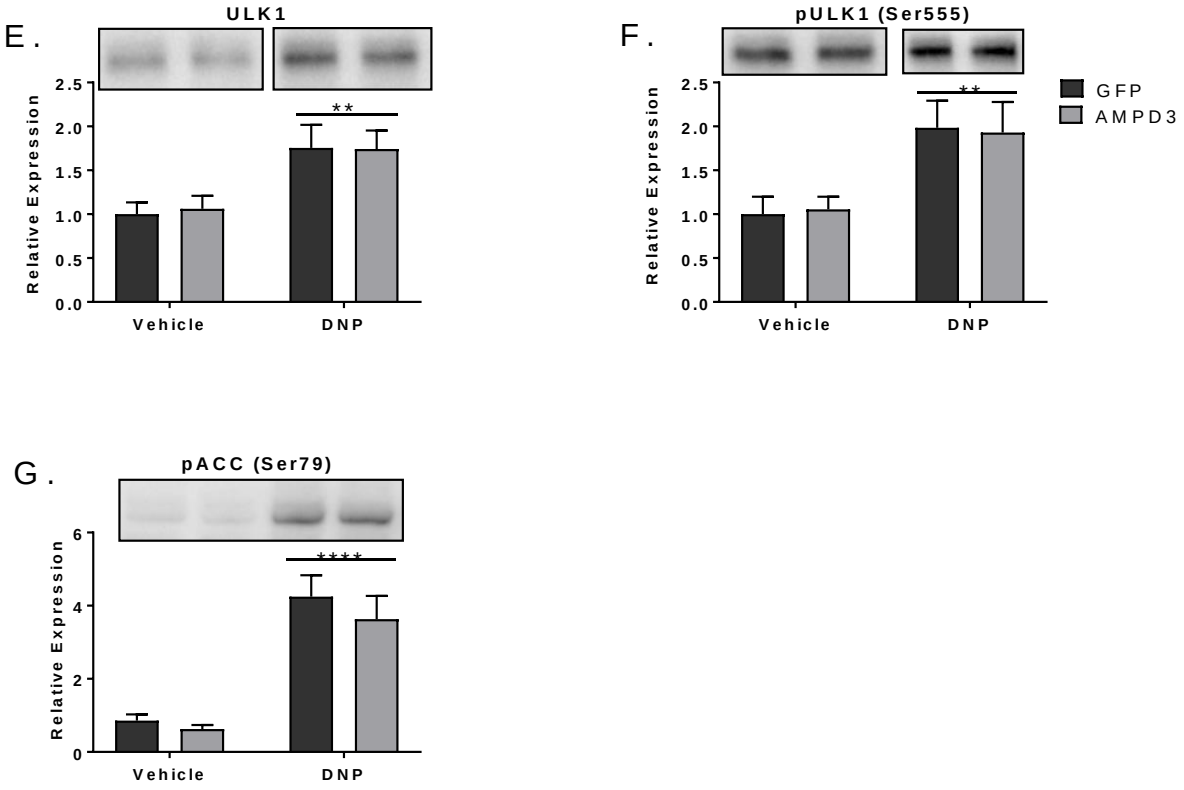

Figure 5. AMPD3 overexpression does not effect phosphorylation of downstream AMPK targets ULK1 and ACC. C2C12 myotubes were transduced with adenovirus encoding either GFP or AMPD3 for 24 hours and treated with 0.6 mM 2,4 dinitrophenol (DNP) or vehicle (methanol) for 1 hour. Proteins were extracted and expression levels were measured by Western Blot. E. Protein expression levels of ULK1. F. Protein expression levels of phosphorylated ULK1 (Ser555). G. Protein expression levels of phosphorylated ACC (Ser79).
**= $p<0.001$, ****= $p<0.0001$

Effects of long-term AMPD3 overexpression on PGC-1α and mitochondrial content.

Changes in mitochondrial content occur in response to repeated increases in PGC-1α content and the transcription, translation, and incorporation of mitochondrial proteins into existing mitochondria [23,73]. Therefore, in order to test the effect of AMPD3 on the activation of PGC-1α and mitochondrial content, we overexpressed AMPD3 and treated cells with a long-term dosage of DNP. To do this we transduced myotubes with adenovirus encoding AMPD3 or GFP, and 24 hours later began a continuous low-dose treatment (100μM) with DNP for 4 days.

We first sought to determine the effect of long-term AMPD3 overexpression and continuous low-dose DNP treatment on the concentration of adenine nucleotides (Figure 6). Overexpressing AMPD3 significantly decreased [ATP] (1.3-fold) in both vehicle and DNP groups compared to GFP (Fig. 6a). The low dose DNP treatment did not result in significant increases [ADP] and no differences were measured between AMPD3 and GFP (Fig. 6b). However, DNP significantly increased [AMP], while AMPD3 overexpression caused a significant main effect decrease in [AMP] (Fig. 6c). AMPD3 overexpression increased [IMP] in both vehicle and DNP groups compared to undetectable in GFP (Fig. 6e). Lastly, AMPD3 groups had significantly less AN+IMP in both vehicle (1.3-fold) and DNP (1.2-fold) groups (Fig. 6f). These results show that long-term overexpression of AMPD3 during continuous low-dose DNP treatment can result in significantly decreased [ATP], [AMP], and the total adenine nucleotide pool (AN+IMP).

Muscle cells typically adapt to decreases in [ATP], such as in Figure 6, by increasing expression of PGC-1α and subsequently increasing mitochondrial biogenesis [23]. Therefore, we measured the activity of the PGC-1α promotor region by transfecting C2C12 myoblasts with plasmids containing 2 kilo-bases of the PGC-1α promotor sequence upstream of the firefly

luciferase protein [29]. Transfected myoblasts were switched to differentiation media, and AMPD3 was overexpressed by adenovirus 24 hours after transfection. On the fifth day of overexpression, myotubes were lysed and luciferase activity was measured (Fig. 7b). Myotubes overexpressing AMPD3 had significantly less luciferase activity compared to those overexpressing GFP ($p<0.005$). These results show that a chronic overexpression of AMPD3 is sufficient to decrease PGC-1α promotor region activity and, since PGC-1α can regulate mitochondrial biogenesis, suggest that AMPD3 could regulate mitochondrial content.

Therefore, we next examined the effects of AMPD3 overexpression on mitochondrial content by treating live myotubes with fluorescent stains specific for mitochondria (MitoTracker green) and nuclei (Hoechst 33343) (Figure 8). Before staining myotubes were treated with adenovirus overexpressing AMPD3 or RFP (control) for 5 days, as well as, a 4-day continuous treatment of 100 μM DNP. After staining we captured fluorescent images of the myotubes and quantified the relative percentage of pixels that emitted green fluorescence as a measure of mitochondrial content. DNP treatment significantly increased the percentage of pixels positive for green fluorescence. However, myotubes overexpressing AMPD3 had significantly less green fluorescence than RFP controls. These findings suggest that DNP treatment for 4 days is capable of increasing mitochondrial content in C2C12 myotubes, but overexpression of AMPD3 can attenuate this response, thus, acting as a negative regulator of mitochondrial content.

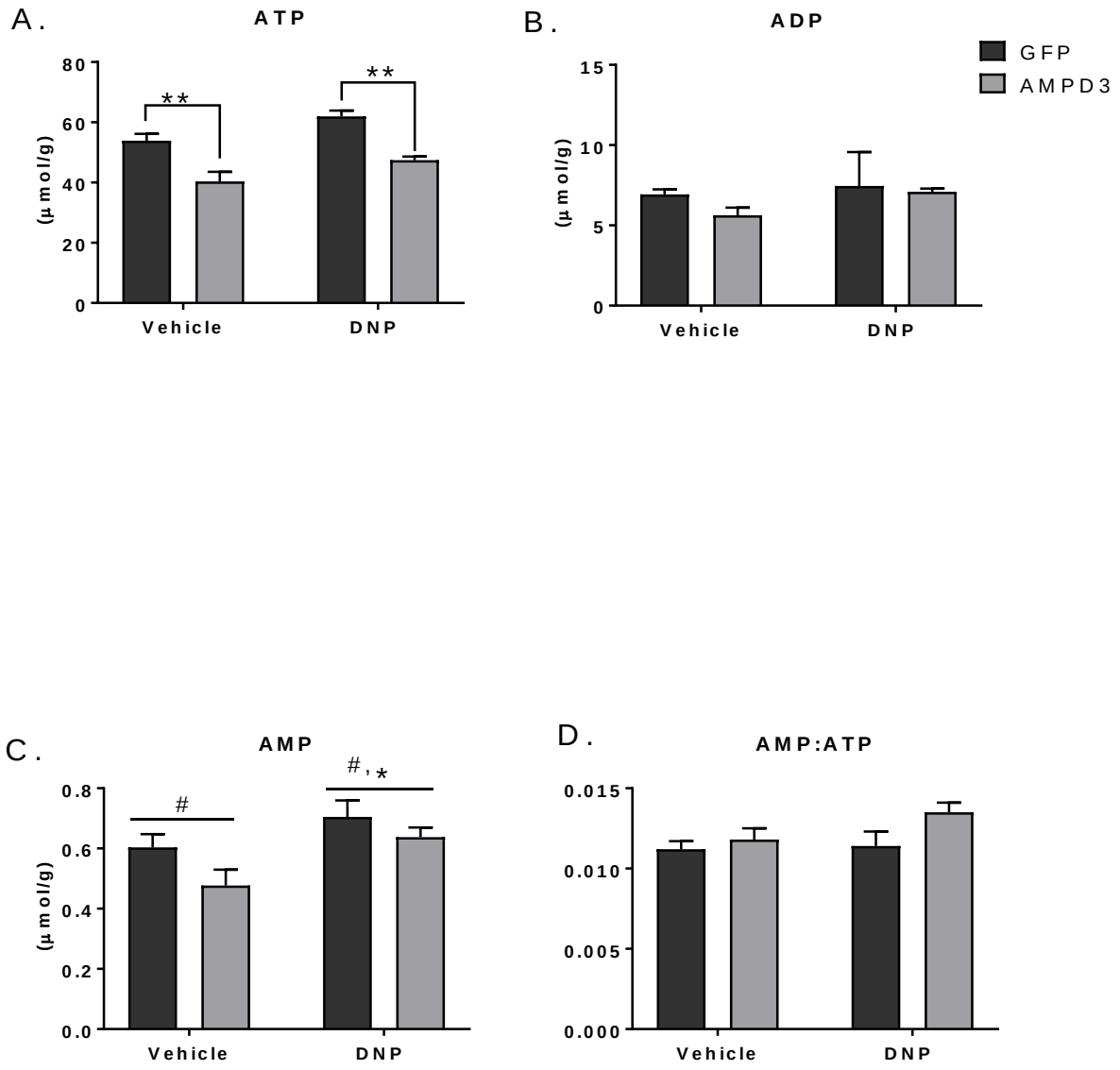

Figure 6. Long-term overexpression of AMPD3 decreases ATP and the total adenine nucleotide pool. C2C12 myotubes were transduced with adenovirus encoding AMPD3 or GFP and then treated with 100µm 2,4 dinitrophenol (DNP) continuously for 4 days. On day 4 of DNP treatment (day 5 of overexpression) nucleotides were extracted and analyzed by UPLC. A-C. Adenine nucleotide concentrations normalized to total protein content. D. The calculated ratio of AMP to ATP.
**= $p<0.001$, *= $p<0.05$, # = main effect of AMPD3 $p=0.05$

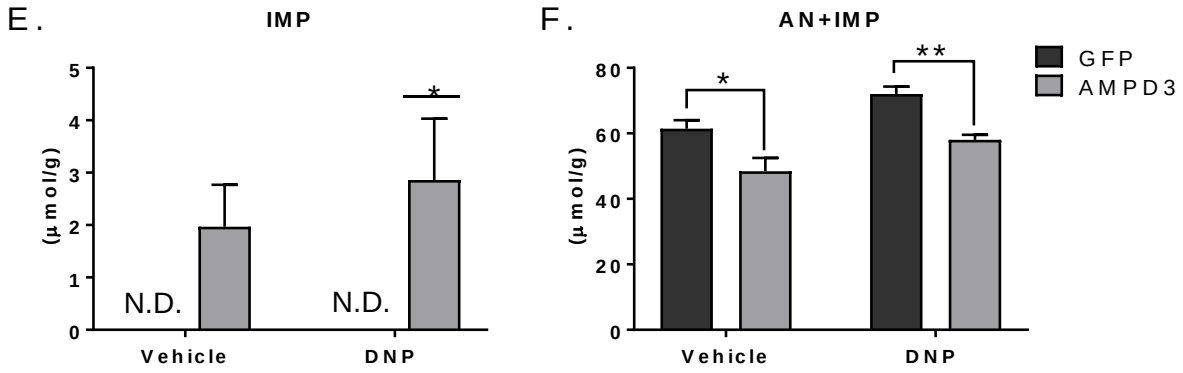

Figure 6. Long-term overexpression of AMPD3 decreases ATP and the total adenine nucleotide pool. C2C12 myotubes were transduced with adenovirus encoding AMPD3 or GFP and then treated with 100µm 2,4 dinitrophenol (DNP) continuously for 4 days. On day 4 of DNP treatment (day 5 of overexpression) nucleotides were extracted and analyzed by UPLC. E. IMP concentrations normalized to total protein content. F. Total adenine nucleotides plus IMP.
*= $p<0.01$, **= $p<0.001$, N.D. = none detected

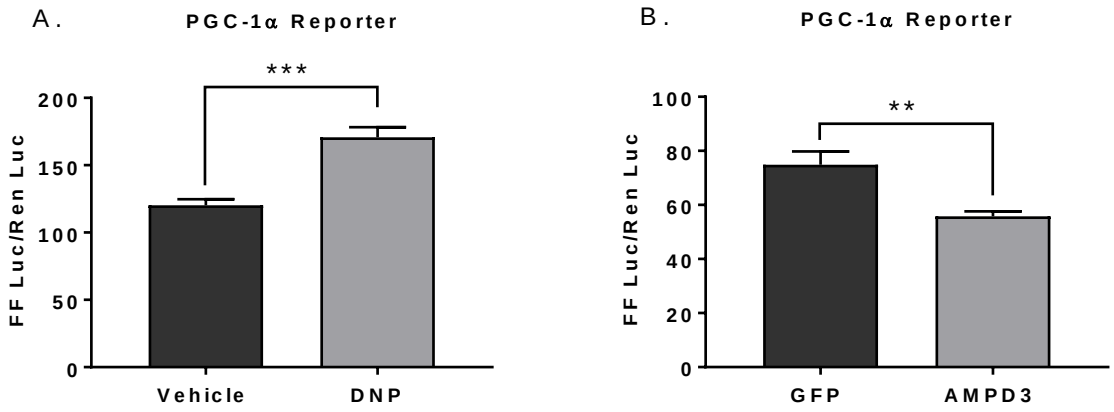

Figure 7. AMPD3 overexpression decreases PGC-1α promotor activity. C2C12 myoblasts were transfected with plasmids containing 2Kb of PGC-1α promotor region encoding luciferase protein. 24 hours after transfection myoblasts were switched to differentiation media. A. Luciferase activity in myotubes after 4 days of treatment with 100μM DNP. B. Luciferase activity in myotubes overexpressing GFP or AMPD3 for 5 days.
=$p<0.005$,*= $p<0.001$

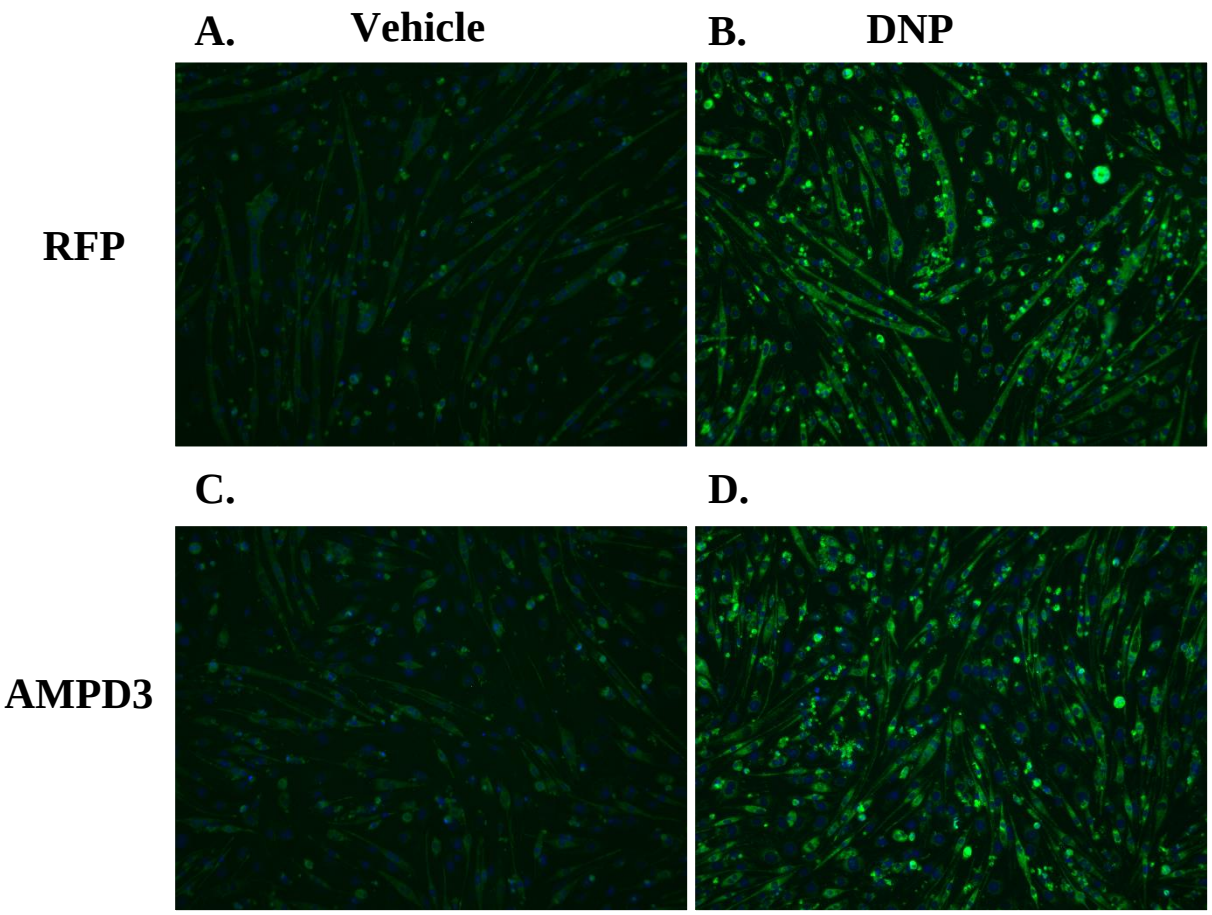

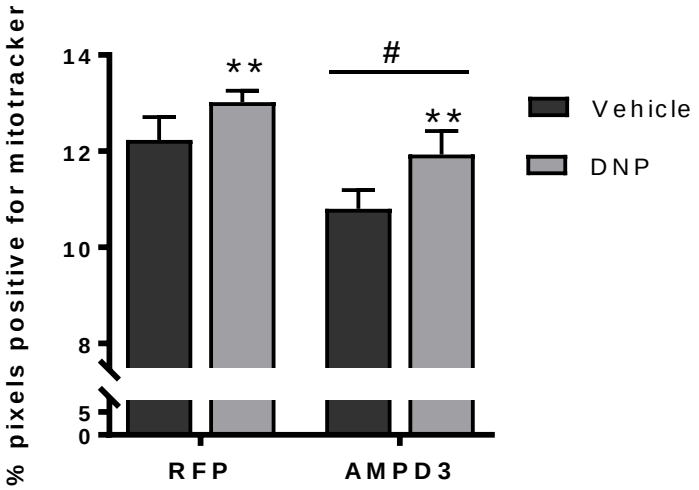

Figure 8. Myotubes overexpressing AMPD3 have less mitochondria. After adenovirus transduction, myotubes were treated with 100μM DNP for 4 days. Mitochondria and nuclei were stained with green and blue fluorescent dyes. Images were captured and percentage of pixels positive for green florescence were quantified using ImageJ software.
**= main effect of DNP $p<0.05$, #= main effect of AMPD3 $p<0.01$

Chapter 5: Discussion

DNP treatment creates an ATP supply/demand mismatch and increases mitochondrial content.

In response to an increase in energy demand such as muscle contractions, or conditions where energy production is impaired such as ischemia or mitochondrial dysfunction, the hydrolysis of ATP will outpace ADP phosphorylation causing an increase in [ADP] [60]. If the energy demanding conditions continue, [AMP] will increase due to the near equilibrium reaction of adenylate kinase (ADP + ADP ↔ ATP+AMP) which is critical to maintain the ADP:ATP ratio and preserve the free energy of ATP hydrolysis [65]. Increasing [AMP] will then activate the AMPD reaction (AMP→IMP+NH_3) and cause an increase in [IMP] [34]. We found that increasing DNP concentrations up to 1 mM caused a curvilinear decrease in [ATP], and increase in [AMP], AMP:ATP, and [IMP]. Interestingly [ADP] peaked at 0.6 mM DNP but then decreased with 0.8 and 1 mM concentrations. This could be the result of the significant decrease in total AN+IMP that occurred during the 0.8 and 1 mM concentrations. All together our results show that treatment with a mitochondrial uncoupler such as DNP is sufficient to decrease cellular energy and create similar energetic profiles that are seen during prolonged or intense exercise [87]. In turn, this causes increases in phosphorylated AMPK (Thr172) (Fig. 5b), PGC-1α promotor region activity (Fig. 7a), and mitochondrial content (Fig. 8). These results agree with an *in vivo* study that found supplementing DNP into rat chow for 28 days could increase the mRNA expression for several genes and proteins involved in mitochondrial biogenesis including PGC-1α , NRF-1, Tfam, citrate synthase, and several other mitochondrial proteins [88].

AMPD3 overexpression during short term energy demand

While the degradation of AMP is critical to preserve cellular free energy during intense muscle contractions or ischemia [60,65], the increase in [AMP] is also important for activating

mitochondrial biogenesis through enhancing phosphorylation of AMPK(Thr172) [25,26,89]. During atrophy AMPD3 expression is significantly increased in skeletal muscle, but whether its overexpression is sufficient to decrease [AMP] and phosphorylation of AMPK(Thr172) were unknown. To test this we used C2C12 myotubes as an *in vitro* model of skeletal muscle and then overexpressed AMPD3 using an adenovirus. During resting conditions [AMP] is low in skeletal muscle [65,86]. Therefore, in order to determine the effect of AMPD3 overexpression, we had to increase [AMP] by creating an energy demand. Our results show that in response to decreases in [ATP], AMPD3 overexpression is sufficient to significantly attenuate increases in [ADP], [AMP], and the AMP:ATP ratio (Figure 2). However, while [AMP] and the AMP:ATP ratio were significantly less in DNP-AMPD3 compared to DNP-GFP, they were still higher than both vehicle groups and this could explain why we only observed a significant main effect when measuring the amount of phosphorylated AMPK(Thr172) (Figure 5). For instance, the concentration of [AMP] increased 2.9-fold from Veh-GFP to DNP-AMPD3 while the AMP:ATP ratio increased 7.2-fold from Veh-GFP to DNP-AMPD3. Not surprisingly this resulted in dramatic increases in the amount of phosphorylated AMPK, which suggests that AMPK is highly sensitive to increases in [AMP] and the AMP:ATP ratio. This could mean that our comparison of phosphorylated AMPK(Thr172) between DNP-GFP and DNP-AMPD3 is a measure of AMPK proteins that are completely phosphorylated to those that are only slightly less phosphorylated. If so, then possibly a DNP concentration between 0.4 and 0.6 mM might have resulted in significantly less phosphorylated AMPK(Thr172) in DNP-AMPD3 vs DNP-GFP.

Apart from measures of phosphorylated AMPK(Thr172) content, we also measured the phosphorylation of several downstream targets of AMPK such as Acetyl CoA Carboxylase (ACC, Ser79) and Unc-51-like kinase 1 (ULK1, Ser555) (Figure 5 E&F). Despite having less

phosphorylated AMPK we did not measure any differences in the amount of phosphorylated ACC and ULK1 between AMPD3 and GFP groups after the DNP treatment. We did however see a significant increase in the phosphorylation of these proteins in myotubes treated with DNP. This agrees with the evidence that these proteins are targeted by AMPK during times of energy demand [61,79,80]. ACC catalyzes the formation of malonyl-CoA from cytosolic acetyl-CoA and therefore functions to inhibit fatty-acid oxidation by increasing cellular malonyl-CoA levels, which inhibits CPT1 and the transport of fatty acids into the mitochondria for β-oxidation[90]. When phosphorylated by AMPK during times of energy demand, ACC becomes inactive and thus fatty acids are oxidized in the mitochondria via β-oxidation to generate ATP. On the other hand, ULK1 is phosphorylated by AMPK on serine 317, 555, and 777 residues which initiates the formation of the autophagosome and protein degradation via autophagy [79,80]. Therefore, while these proteins are downstream targets of AMPK and thus can be considered a measure of AMPK activation, they are not known to regulate mitochondrial biogenesis and do not rule out the possibility that AMPK targets that do contribute to mitochondrial biogenesis, such as PGC-1α , could be less phosphorylated when AMPD3 is overexpressed. Further measures of AMPK activity, such as direct AMPK enzyme activity and phosphorylation of PGC-1α on AMPK targeted residues, should be measured to further determine AMPK activity when AMPD3 is overexpressed.

The purpose of our study was similar to another that investigated AMP metabolism and the activation of AMPK in HEK293T kidney cells [91]. In this study by Plaideau et al., HEK293T cells were transfected with plasmids encoding AMPD1, AMPD2, and cytosolic 5' nucleotidase IA (cN-IA). They then serum starved the HEK293T cells for 4 hours with DMEM containing low glucose (1mg/ml) and incubated with or without the ATP synthase inhibitor oligomycin.

They found that serum starvation using a low glucose concentration along with oligomycin treatment was sufficient to increase [ADP], [AMP], AMP:ATP ratio, and the activity of AMPK. Transfecting plasmids that encode AMPD1, AMPD2, and cN-IA resulted in attenuated increases in [ADP], [AMP], AMP:ATP ratio, and the activity of AMPK. However, only cells transfected with cN-IA expressing plasmids had significant reductions in these measures. The inability of AMPD1 and AMPD2 transfection to result in significant decreases in [ADP], [AMP], and AMPK activity could be explained by the fact that AMPD1 and AMPD2 are not typically expressed in kidney cells [92].

Increased Purine Nucleotide Cycle activity

The purine nucleotide cycle (PNC) has several important physiological functions including: 1) regulation of the relative AMP, ADP, and ATP levels through the removal of AMP to IMP [87], 2) regulation of phosphofructokinase activity by elevations in ammonia [93], 3) generation of citric acid cycle intermediates [83,94], and 4) deamination of amino acids for oxidative metabolism [95]. The activity of the PNC is dependent on the rate of AMPD activity, and therefore AMPD3 overexpression could potentially lead to increased PNC activity, aspartic acid catabolism, and citric acid cycle flux. In fact, a recent study found that AMPD3 overexpression in C2C12 myotubes can significantly increase rates of aspartic acid oxidation, fatty acid oxidation, and oxygen consumption during electrical pulse stimulation [96]. We found that a 1 hour treatment with DNP increased aspartic acid concentrations significantly, and following a 1 hour recovery period they return back to resting levels (Figure 4). The dramatic increase in aspartic acid and IMP concentrations after DNP treatment suggests that the PNC is either slower or unable to match the rates of amino acid and AMP catabolism during the energy demand. The

return of aspartic acid and IMP concentrations to values similar to vehicle groups suggests that during the recovery the PNC is active.

AMPD3 overexpression during long term energy demand

A downstream target of AMPK is the transcriptional co-activator PGC-1α, which is an established activator of mitochondrial biogenesis in skeletal muscle. AMPK has been shown to phosphorylate PGC-1α on threonine 177 and serine 538 residues which will stimulate PGC-1α to translocate to the nucleus where it will interact with transcription factors such as PPAR and NRF-1 [23,29]. These transcription factors regulate the gene expression of several nuclear encoded mitochondrial proteins and upon binding by PGC-1α increase their transcription. PGC-1α has also been shown to increase the transcription of its own gene sequence after phosphorylation by AMPK [27]. Therefore by measuring the promotor region activity of PGC-1α, we can acquire a sensitive indirect measure of PGC-1α expression and activity. We found that AMPD3 overexpression for 5 days decreases PGC-1α promotor region activity (Fig. 7b), which could also suggest that less cytosolic PGC-1α translocated to the nucleus after phosphorylation by AMPK. PGC-1α can also be activated by deacetylation by SIRT1. Therefore, further measures of decreased PGC-1α activation, such as less mRNA and protein content, phosphorylation and acetylation on AMPK or SIRT1 targeted residues, and decreases in the ratio of nuclear to cytosolic PGC-1α, would add convincing evidence to support AMPD3 regulation of PGC-1α.

Our main hypothesis is that AMPD3 overexpression can negatively regulate mitochondrial content in skeletal muscle. By quantifying the relative percentage of mitochondrial fluorescence in images from myotubes treated for four days with 100 μM DNP, we found significant decreases in percentages of fluorescence when AMPD3 was overexpressed compared to RFP (Figure 8). This finding supports our hypothesis that AMPD3 can negatively regulate

mitochondrial content in skeletal muscle, however, several other measures of mitochondrial content are needed to confirm this finding because mitochondrial are may not translate to mitochondrial enzymes or oxidative capacity. Other measures of mitochondrial content that could be performed include: 1) mRNA and protein content for mitochondrial proteins such as citrate synthase, succinate dehydrogenase, and oxidative phosphorylation enzymes, 2) incorporation of radiolabeled amino acids into mitochondrial proteins to determine rates of mitochondrial protein synthesis, 3) mitochondrial DNA content relative to nuclear DNA, and 4) maximal oxygen consumption.

In conclusion, we found that a short-term overexpression of AMPD3 can significantly attenuate increases in [AMP] and phosphorylation of AMPK(Thr172) during energy demand. Furthermore, a long-term overexpression of AMPD3 can significantly decrease PGC-1α promotor region activity and mitochondrial content in C2C12 myotubes. These findings indicate that AMPD3 is possibly a novel regulator of mitochondrial content in skeletal muscle. Selective inhibition of AMPD3 in skeletal muscles undergoing atrophy could potentially preserve mitochondrial content and muscle function. This may allow patients to maintain exercise capacity and activities of daily living, combat reductions in muscle mass, and hopefully delay mortality.

References

1. Adamo, M. L. & Farrar, R. P. Resistance training, and IGF involvement in the maintenance of muscle mass during the aging process. *Ageing Res. Rev.* **5,** 310–331 (2006).
2. Rogers, M. A. & Evans, W. J. Changes in skeletal muscle with aging: effects of exercise training. *Exerc. Sport Sci. Rev.* **21,** 65–102 (1993).
3. Kauffman, F. C. & Albuquerque, E. X. Effect of ischemia and denervation on metabolism of fast and slow mammalian skeletal muscle. *Exp. Neurol.* **28,** 46–63 (1970).
4. Lu, D. X., Huang, S. K. & Carlson, B. M. Electron microscopic study of long-term denervated rat skeletal muscle. *Anat. Rec.* **248,** 355–365 (1997).
5. Pellegrino, C. & Franzini, C. AN ELECTRON MICROSCOPE STUDY OF DENERVATION ATROPHY IN RED AND WHITE SKELETAL MUSCLE FIBERS. *J. Cell Biol.* **17,** 327–349 (1963).
6. Guerrero, N. *et al.* Premature loss of muscle mass and function in type 2 diabetes. *Diabetes Res. Clin. Pract.* **117,** 32–38 (2016).
7. Johansen, K. L. *et al.* Muscle atrophy in patients receiving hemodialysis: effects on muscle strength, muscle quality, and physical function. *Kidney Int.* **63,** 291–297 (2003).
8. von Haehling, S. The wasting continuum in heart failure: from sarcopenia to cachexia. *Proc. Nutr. Soc.* **74,** 367–377 (2015).
9. von Haehling, S., Anker, M. S. & Anker, S. D. Prevalence and clinical impact of cachexia in chronic illness in Europe, USA, and Japan: facts and numbers update 2016. *J. Cachexia Sarcopenia Muscle* **7,** 507–509 (2016).

10. Metter, E. J., Talbot, L. A., Schrager, M. & Conwit, R. Skeletal muscle strength as a predictor of all-cause mortality in healthy men. *J. Gerontol. A. Biol. Sci. Med. Sci.* **57,** B359-365 (2002).
11. Rantanen, T. *et al.* Muscle strength and body mass index as long-term predictors of mortality in initially healthy men. *J. Gerontol. A. Biol. Sci. Med. Sci.* **55,** M168-173 (2000).
12. Zhou, X. *et al.* Reversal of cancer cachexia and muscle wasting by ActRIIB antagonism leads to prolonged survival. *Cell* **142,** 531–543 (2010).
13. Fontes-Oliveira, C. C. *et al.* Mitochondrial and sarcoplasmic reticulum abnormalities in cancer cachexia: altered energetic efficiency? *Biochim. Biophys. Acta* **1830,** 2770–2778 (2013).
14. Constantinou, C. *et al.* Nuclear magnetic resonance in conjunction with functional genomics suggests mitochondrial dysfunction in a murine model of cancer cachexia. *Int. J. Mol. Med.* **27,** 15–24 (2011).
15. Fewell, J. G. & Moerland, T. S. Responses of mouse fast and slow skeletal muscle to streptozotocin diabetes: myosin isoenzymes and phosphorous metabolites. *Mol. Cell. Biochem.* **148,** 147–154 (1995).
16. Zhao, C.-R., Shang, L., Wang, W. & Jacobs, D. O. Myocellular creatine and creatine transporter serine phosphorylation after starvation. *J. Surg. Res.* **105,** 10–16 (2002).
17. Roberts, B. M., Frye, G. S., Ahn, B., Ferreira, L. F. & Judge, A. R. Cancer cachexia decreases specific force and accelerates fatigue in limb muscle. *Biochem. Biophys. Res. Commun.* **435,** 488–492 (2013).
18. Wicks, K. L. & Hood, D. A. Mitochondrial adaptations in denervated muscle: relationship to muscle performance. *Am. J. Physiol.* **260,** C841-850 (1991).

19. Korpelainen, R. *et al.* Exercise capacity and mortality - a follow-up study of 3033 subjects referred to clinical exercise testing. *Ann. Med.* **48,** 359–366 (2016).
20. Benatti, F. B. & Pedersen, B. K. Exercise as an anti-inflammatory therapy for rheumatic diseases-myokine regulation. *Nat. Rev. Rheumatol.* **11,** 86–97 (2015).
21. Bowen, T. S., Schuler, G. & Adams, V. Skeletal muscle wasting in cachexia and sarcopenia: molecular pathophysiology and impact of exercise training. *J. Cachexia Sarcopenia Muscle* **6,** 197–207 (2015).
22. Ikizler, T. A. Exercise as an anabolic intervention in patients with end-stage renal disease. *J. Ren. Nutr. Off. J. Counc. Ren. Nutr. Natl. Kidney Found.* **21,** 52–56 (2011).
23. Hood, D. A., Tryon, L. D., Carter, H. N., Kim, Y. & Chen, C. C. W. Unravelling the mechanisms regulating muscle mitochondrial biogenesis. *Biochem. J.* **473,** 2295–2314 (2016).
24. Romanello, V. & Sandri, M. Mitochondrial Quality Control and Muscle Mass Maintenance. *Front. Physiol.* **6,** 422 (2015).
25. Bergeron, R. *et al.* Chronic activation of AMP kinase results in NRF-1 activation and mitochondrial biogenesis. *Am. J. Physiol. Endocrinol. Metab.* **281,** E1340-1346 (2001).
26. Winder, W. W. *et al.* Activation of AMP-activated protein kinase increases mitochondrial enzymes in skeletal muscle. *J. Appl. Physiol. Bethesda Md 1985* **88,** 2219–2226 (2000).
27. Handschin, C., Rhee, J., Lin, J., Tarr, P. T. & Spiegelman, B. M. An autoregulatory loop controls peroxisome proliferator-activated receptor gamma coactivator 1alpha expression in muscle. *Proc. Natl. Acad. Sci. U. S. A.* **100,** 7111–7116 (2003).
28. Hardie, D. G., Ross, F. A. & Hawley, S. A. AMPK: a nutrient and energy sensor that maintains energy homeostasis. *Nat. Rev. Mol. Cell Biol.* **13,** 251–262 (2012).

29. Jäger, S., Handschin, C., St-Pierre, J. & Spiegelman, B. M. AMP-activated protein kinase (AMPK) action in skeletal muscle via direct phosphorylation of PGC-1α lpha. *Proc. Natl. Acad. Sci. U. S. A.* **104,** 12017–12022 (2007).
30. Brault, J. J., Jespersen, J. G. & Goldberg, A. L. Peroxisome proliferator-activated receptor gamma coactivator 1alpha or 1beta overexpression inhibits muscle protein degradation, induction of ubiquitin ligases, and disuse atrophy. *J. Biol. Chem.* **285,** 19460–19471 (2010).
31. Lecker, S. H. *et al.* Multiple types of skeletal muscle atrophy involve a common program of changes in gene expression. *FASEB J. Off. Publ. Fed. Am. Soc. Exp. Biol.* **18,** 39–51 (2004).
32. Sacheck, J. M. *et al.* Rapid disuse and denervation atrophy involve transcriptional changes similar to those of muscle wasting during systemic diseases. *FASEB J. Off. Publ. Fed. Am. Soc. Exp. Biol.* **21,** 140–155 (2007).
33. Fortuin, F. D., Morisaki, T. & Holmes, E. W. Subunit composition of AMPD varies in response to changes in AMPD1 and AMPD3 gene expression in skeletal muscle. *Proc. Assoc. Am. Physicians* **108,** 329–333 (1996).
34. Meyer, R. A. & Terjung, R. L. AMP deamination and IMP reamination in working skeletal muscle. *Am. J. Physiol.* **239,** C32-38 (1980).
35. Lecker, S. H., Solomon, V., Mitch, W. E. & Goldberg, A. L. Muscle protein breakdown and the critical role of the ubiquitin-proteasome pathway in normal and disease states. *J. Nutr.* **129,** 227S–237S (1999).
36. Glass, D. J. Signalling pathways that mediate skeletal muscle hypertrophy and atrophy. *Nat. Cell Biol.* **5,** 87–90 (2003).

37. Latres, E. *et al.* Insulin-like growth factor-1 (IGF-1) inversely regulates atrophy-induced genes via the phosphatidylinositol 3-kinase/Akt/mammalian target of rapamycin (PI3K/Akt/mTOR) pathway. *J. Biol. Chem.* **280,** 2737–2744 (2005).
38. Zhao, J., Brault, J. J., Schild, A. & Goldberg, A. L. Coordinate activation of autophagy and the proteasome pathway by FoxO transcription factor. *Autophagy* **4,** 378–380 (2008).
39. Sandri, M. *et al.* PGC-1α lpha protects skeletal muscle from atrophy by suppressing FoxO3 action and atrophy-specific gene transcription. *Proc. Natl. Acad. Sci. U. S. A.* **103,** 16260–16265 (2006).
40. Cai, D. *et al.* IKKbeta/NF-kappaB activation causes severe muscle wasting in mice. *Cell* **119,** 285–298 (2004).
41. Sartori, R. *et al.* Smad2 and 3 transcription factors control muscle mass in adulthood. *Am. J. Physiol. Cell Physiol.* **296,** C1248-1257 (2009).
42. Wing, S. S. & Goldberg, A. L. Glucocorticoids activate the ATP-ubiquitin-dependent proteolytic system in skeletal muscle during fasting. *Am. J. Physiol.* **264,** E668-676 (1993).
43. Rock, K. L. *et al.* Inhibitors of the proteasome block the degradation of most cell proteins and the generation of peptides presented on MHC class I molecules. *Cell* **78,** 761–771 (1994).
44. Sandri, M. Protein breakdown in muscle wasting: role of autophagy-lysosome and ubiquitin-proteasome. *Int. J. Biochem. Cell Biol.* **45,** 2121–2129 (2013).
45. Gronostajski, R. M., Pardee, A. B. & Goldberg, A. L. The ATP dependence of the degradation of short- and long-lived proteins in growing fibroblasts. *J. Biol. Chem.* **260,** 3344–3349 (1985).

46. St John, A. C. & Goldberg, A. L. Effects of reduced energy production on protein degradation, guanosine tetraphosphate, and RNA synthesis in Escherichia coli. *J. Biol. Chem.* **253,** 2705–2711 (1978).

47. Hershko, A. & Ciechanover, A. The ubiquitin system for protein degradation. *Annu. Rev. Biochem.* **61,** 761–807 (1992).

48. Bailey, J. L. *et al.* The acidosis of chronic renal failure activates muscle proteolysis in rats by augmenting transcription of genes encoding proteins of the ATP-dependent ubiquitin-proteasome pathway. *J. Clin. Invest.* **97,** 1447–1453 (1996).

49. Eisenmann, J. C. *et al.* Aerobic fitness, body mass index, and CVD risk factors among adolescents: the Québec family study. *Int. J. Obes. 2005* **29,** 1077–1083 (2005).

50. Ladenvall, P. *et al.* Low aerobic capacity in middle-aged men associated with increased mortality rates during 45 years of follow-up. *Eur. J. Prev. Cardiol.* **23,** 1557–1564 (2016).

51. Putti, R., Migliaccio, V., Sica, R. & Lionetti, L. Skeletal Muscle Mitochondrial Bioenergetics and Morphology in High Fat Diet Induced Obesity and Insulin Resistance: Focus on Dietary Fat Source. *Front. Physiol.* **6,** 426 (2015).

52. Mul, J. D., Stanford, K. I., Hirshman, M. F. & Goodyear, L. J. Exercise and Regulation of Carbohydrate Metabolism. *Prog. Mol. Biol. Transl. Sci.* **135,** 17–37 (2015).

53. Carson, J. A., Hardee, J. P. & VanderVeen, B. N. The emerging role of skeletal muscle oxidative metabolism as a biological target and cellular regulator of cancer-induced muscle wasting. *Semin. Cell Dev. Biol.* **54,** 53–67 (2016).

54. Morley, J. E., Thomas, D. R. & Wilson, M.-M. G. Cachexia: pathophysiology and clinical relevance. *Am. J. Clin. Nutr.* **83,** 735–743 (2006).

55. Perry, B. D. *et al.* Muscle atrophy in patients with Type 2 Diabetes Mellitus: roles of inflammatory pathways, physical activity and exercise. *Exerc. Immunol. Rev.* **22,** 94–109 (2016).
56. Kouidi, E. *et al.* The effects of exercise training on muscle atrophy in haemodialysis patients. *Nephrol. Dial. Transplant. Off. Publ. Eur. Dial. Transpl. Assoc. - Eur. Ren. Assoc.* **13,** 685–699 (1998).
57. Mootha, V. K. *et al.* PGC-1α lpha-responsive genes involved in oxidative phosphorylation are coordinately downregulated in human diabetes. *Nat. Genet.* **34,** 267–273 (2003).
58. Sayer, A. A. *et al.* Type 2 diabetes, muscle strength, and impaired physical function: the tip of the iceberg? *Diabetes Care* **28,** 2541–2542 (2005).
59. Yokoi, H. & Yanagita, M. Decrease of muscle volume in chronic kidney disease: the role of mitochondria in skeletal muscle. *Kidney Int.* **85,** 1258–1260 (2014).
60. Sahlin, K. & Broberg, S. Adenine nucleotide depletion in human muscle during exercise: causality and significance of AMP deamination. *Int. J. Sports Med.* **11 Suppl 2,** S62-67 (1990).
61. Cantó, C. *et al.* Interdependence of AMPK and SIRT1 for metabolic adaptation to fasting and exercise in skeletal muscle. *Cell Metab.* **11,** 213–219 (2010).
62. Ojuka, E. O., Jones, T. E., Han, D.-H., Chen, M. & Holloszy, J. O. Raising Ca2+ in L6 myotubes mimics effects of exercise on mitochondrial biogenesis in muscle. *FASEB J. Off. Publ. Fed. Am. Soc. Exp. Biol.* **17,** 675–681 (2003).
63. Wu, H. *et al.* Regulation of mitochondrial biogenesis in skeletal muscle by CaMK. *Science* **296,** 349–352 (2002).

64. Costford, S. R. *et al.* Skeletal muscle NAMPT is induced by exercise in humans. *Am. J. Physiol. Endocrinol. Metab.* **298,** E117-126 (2010).

65. Hancock, C. R., Brault, J. J. & Terjung, R. L. Protecting the cellular energy state during contractions: role of AMP deaminase. *J. Physiol. Pharmacol. Off. J. Pol. Physiol. Soc.* **57 Suppl 10,** 17–29 (2006).

66. Narkar, V. A. *et al.* AMPK and PPARdelta agonists are exercise mimetics. *Cell* **134,** 405–415 (2008).

67. O'Neill, H. M. *et al.* AMP-activated protein kinase (AMPK) beta1beta2 muscle null mice reveal an essential role for AMPK in maintaining mitochondrial content and glucose uptake during exercise. *Proc. Natl. Acad. Sci. U. S. A.* **108,** 16092–16097 (2011).

68. Freyssenet, D., Irrcher, I., Connor, M. K., Di Carlo, M. & Hood, D. A. Calcium-regulated changes in mitochondrial phenotype in skeletal muscle cells. *Am. J. Physiol. Cell Physiol.* **286,** C1053-1061 (2004).

69. Schudt, C., Gaertner, U., Dölken, G. & Pette, D. Calcium-related changes of enzyme activities in energy metabolism of cultured embryonic chick myoblasts and myotubes. *Eur. J. Biochem.* **60,** 579–586 (1975).

70. Menzies, K. J., Singh, K., Saleem, A. & Hood, D. A. Sirtuin 1-mediated effects of exercise and resveratrol on mitochondrial biogenesis. *J. Biol. Chem.* **288,** 6968–6979 (2013).

71. Yuan, Y. *et al.* Regulation of SIRT1 in aging: Roles in mitochondrial function and biogenesis. *Mech. Ageing Dev.* **155,** 10–21 (2016).

72. Fulco, M. *et al.* Glucose restriction inhibits skeletal myoblast differentiation by activating SIRT1 through AMPK-mediated regulation of Nampt. *Dev. Cell* **14,** 661–673 (2008).

73. Pilegaard, H., Saltin, B. & Neufer, P. D. Exercise induces transient transcriptional activation of the PGC-1α lpha gene in human skeletal muscle. *J. Physiol.* **546,** 851–858 (2003).
74. Uguccioni, G. & Hood, D. A. The importance of PGC-1α in contractile activity-induced mitochondrial adaptations. *Am. J. Physiol. Endocrinol. Metab.* **300,** E361-371 (2011).
75. Calvo, J. A. *et al.* Muscle-specific expression of PPARgamma coactivator-1alpha improves exercise performance and increases peak oxygen uptake. *J. Appl. Physiol. Bethesda Md 1985* **104,** 1304–1312 (2008).
76. Puigserver, P. *et al.* A cold-inducible coactivator of nuclear receptors linked to adaptive thermogenesis. *Cell* **92,** 829–839 (1998).
77. Lin, J. *et al.* Defects in adaptive energy metabolism with CNS-linked hyperactivity in PGC-1α lpha null mice. *Cell* **119,** 121–135 (2004).
78. Bollinger, L. M., Powell, J. J. S., Houmard, J. A., Witczak, C. A. & Brault, J. J. Skeletal muscle myotubes in severe obesity exhibit altered ubiquitin-proteasome and autophagic/lysosomal proteolytic flux. *Obes. Silver Spring Md* **23,** 1185–1193 (2015).
79. Kim, J., Kundu, M., Viollet, B. & Guan, K.-L. AMPK and mTOR regulate autophagy through direct phosphorylation of Ulk1. *Nat. Cell Biol.* **13,** 132–141 (2011).
80. Bach, M., Larance, M., James, D. E. & Ramm, G. The serine/threonine kinase ULK1 is a target of multiple phosphorylation events. *Biochem. J.* **440,** 283–291 (2011).
81. Lee, I. H. *et al.* A role for the NAD-dependent deacetylase Sirt1 in the regulation of autophagy. *Proc. Natl. Acad. Sci. U. S. A.* **105,** 3374–3379 (2008).
82. Lowenstein, J. M. The purine nucleotide cycle revisited [corrected]. *Int. J. Sports Med.* **11 Suppl 2,** S37-46 (1990).

83. Flanagan, W. F., Holmes, E. W., Sabina, R. L. & Swain, J. L. Importance of purine nucleotide cycle to energy production in skeletal muscle. *Am. J. Physiol.* **251,** C795-802 (1986).

84. Sabina, R. L. *et al.* Myoadenylate deaminase deficiency. Functional and metabolic abnormalities associated with disruption of the purine nucleotide cycle. *J. Clin. Invest.* **73,** 720–730 (1984).

85. Jagoe, R. T., Lecker, S. H., Gomes, M. & Goldberg, A. L. Patterns of gene expression in atrophying skeletal muscles: response to food deprivation. *FASEB J. Off. Publ. Fed. Am. Soc. Exp. Biol.* **16,** 1697–1712 (2002).

86. Brault, J. J., Pizzimenti, N. M., Dentel, J. N. & Wiseman, R. W. Selective inhibition of ATPase activity during contraction alters the activation of p38 MAP kinase isoforms in skeletal muscle. *J. Cell. Biochem.* **114,** 1445–1455 (2013).

87. Tullson, P. C. & Terjung, R. L. Adenine nucleotide metabolism in contracting skeletal muscle. *Exerc. Sport Sci. Rev.* **19,** 507–537 (1991).

88. Schlagowski, A. I. *et al.* Mitochondrial uncoupling reduces exercise capacity despite several skeletal muscle metabolic adaptations. *J. Appl. Physiol. Bethesda Md 1985* **116,** 364–375 (2014).

89. Hardie, D. G. AMPK--sensing energy while talking to other signaling pathways. *Cell Metab.* **20,** 939–952 (2014).

90. Winder, W. W. Malonyl-CoA--regulator of fatty acid oxidation in muscle during exercise. *Exerc. Sport Sci. Rev.* **26,** 117–132 (1998).

91. Plaideau, C. *et al.* Overexpression of AMP-metabolizing enzymes controls adenine nucleotide levels and AMPK activation in HEK293T cells. *FASEB J. Off. Publ. Fed. Am. Soc. Exp. Biol.* **26,** 2685–2694 (2012).
92. Gross, M. Molecular biology of AMP deaminase deficiency. *Pharm. World Sci. PWS* **16,** 55–61 (1994).
93. Abrahams, S. L. & Younathan, E. S. Modulation of the kinetic properties of phosphofructokinase by ammonium ions. *J. Biol. Chem.* **246,** 2464–2467 (1971).
94. Aragón, J. J., Tornheim, K., Goodman, M. N. & Lowenstein, J. M. Replenishment of citric acid cycle intermediates by the purine nucleotide cycle in rat skeletal muscle. *Curr. Top. Cell. Regul.* **18,** 131–149 (1981).
95. Felig, P. & Wahren, J. Amino acid metabolism in exercising man. *J. Clin. Invest.* **50,** 2703–2714 (1971).
96. Hong, S. *et al.* Dissociation of muscle insulin sensitivity from exercise endurance in mice by HDAC3 depletion. *Nat. Med.* **23,** 223–234 (2017).